

---

# Order and Chaos: NTK views on DNN Normalization, Checkerboard and Boundary Artifacts

---

**Arthur Jacot**

Ecole Polytechnique Fédérale de Lausanne  
arthur.jacot@epfl.ch

**Franck Gabriel**

Ecole Polytechnique Fédérale de Lausanne  
franck.gabriel@epfl.ch

**François Ged**

Ecole Polytechnique Fédérale de Lausanne  
francois.ged@epfl.ch

**Clément Hongler**

Ecole Polytechnique Fédérale de Lausanne  
clement.hongler@epfl.ch

## Abstract

We analyze architectural features of Deep Neural Networks (DNNs) using the so-called Neural Tangent Kernel (NTK), which describes the training and generalization of DNNs in the infinite-width setting. In this setting, we show that for fully-connected DNNs, as the depth grows, two regimes appear: *order*, where the (scaled) NTK converges to a constant, and *chaos*, where it converges to a Kronecker delta. Extreme order slows down training while extreme chaos hinders generalization. Using the scaled ReLU as a nonlinearity, we end up in the ordered regime. In contrast, Layer Normalization brings the network into the chaotic regime. We observe a similar effect for Batch Normalization (BN) applied after the last nonlinearity. We uncover the same order and chaos modes in Deep Deconvolutional Networks (DC-NNs). Our analysis explains the appearance of so-called checkerboard patterns and border artifacts. Moving the network into the chaotic regime prevents checkerboard patterns; we propose a graph-based parametrization which eliminates border artifacts; finally, we introduce a new layer-dependent learning rate to improve the convergence of DC-NNs. We illustrate our findings on DCGANs: the ordered regime leads to a collapse of the generator to a checkerboard mode, which can be avoided by tuning the nonlinearity to reach the chaotic regime. As a result, we are able to obtain good quality samples for DCGANs without BN.

## 1 Introduction

The training of Deep Neural Networks (DNN) involves a great variety of architecture choices. It is therefore crucial to find tools to understand their effects and to compare them. For example, Batch Normalization (BN) [10] has proven to be crucial in the training of DNNs but remains ill-understood. While BN was initially introduced to solve the problem of “covariate shift”, recent results [24] suggest an effect on the smoothness of the loss surface. Some alternatives to BN have been proposed [17, 23, 14], yet it remains difficult to compare them theoretically. Recent theoretical results [27] suggest some relation to the transition from “order” to “chaos” observed as the depth of the NN goes to infinity [21, 6, 28].

The impact of architecture is very apparent in GANs [9]: their results are heavily affected by the architecture of the generator and discriminator [22, 29, 4, 13] and the training may fail without BN [3, 25].

Recently, there has been important advances [11, 7, 1] in the understanding of the training of DNNs when the number of neurons in each hidden layer is very large. These results give new tools to study

the asymptotic effect of BN. In particular, the Neural Tangent Kernel (NTK) [11] illustrates the effect of architecture on the training of DNNs and also describes their loss surface [12]. The NTK can easily be extended to Convolutional Neural Networks (CNNs) and other architectures [26, 2], hence allowing comparison. Recently the order/chaos transition has been extended to the NTK in [? ?].

## 1.1 Our Contributions

We describe how the NTK is affected by the “order” and “chaos” regimes [21, 6, 28]. For fully-connected networks, the scaled NTK converges to a constant in the ordered regime and to a Kronecker delta in the chaotic regime. In deconvolutional networks (DC-NNs), a similar transition takes place: the ordered regime features checkerboard patterns [19] and the chaotic regime features a (translation invariant) Kronecker delta.

We then show that different normalization techniques such as Layer Normalization, Batch Normalization and our proposed Nonlinearity Normalization allows the DNN to avoid the ordered regime.

Besides, we prove that the traditional parametrization of DC-NNs leads to border effects in the NTK and we propose a simple solution suggesting a new Graph-Based parametrization. At last, the effect of the number of channels on the NTK is discussed, giving a theoretical motivation for decreasing the number of channels after each upsampling. We show that using a layer-dependent learning rate allows to balance the contributions of the layers to the learning.

Finally, we demonstrate our findings numerically on DC-GANs: we show that in the ordered regime, the generator collapses to a checkerboard mode. We show how a basic DC-GAN can be effectively trained and avoid this mode collapse: by proper hyperparameter tuning, nonlinearity normalization, parametrization and learning rate choices, without using batch normalization, we are able to reach the chaotic regime and to get good quality samples from a very simple DC-NN generator.

## 2 Fully-Connected Neural Networks

The first type of architecture we consider are deep Fully-Connected Neural Networks (FC-NNs). An FC-NN  $\mathbb{R}^{n_0} \rightarrow \mathbb{R}^{n_L}$  with nonlinearity  $\sigma : \mathbb{R} \rightarrow \mathbb{R}$  consists of  $L + 1$  layers ( $L - 1$  hidden layers), respectively containing  $n_0, n_1, \dots, n_L$  neurons. The parameters are the connection weight matrices  $W^{(\ell)} \in \mathbb{R}^{n_{\ell+1} \times n_\ell}$  and bias vectors  $b^{(\ell)} \in \mathbb{R}^{n_{\ell+1}}$  for  $\ell = 0, 1, \dots, L - 1$ . Following [11], the network parameters are aggregated into a single vector  $\theta \in \mathbb{R}^P$  and initialized using iid standard Gaussians  $\mathcal{N}(0, 1)$ . For  $\theta \in \mathbb{R}^P$ , the DNN network function  $f_\theta : \mathbb{R}^{n_0} \rightarrow \mathbb{R}^{n_L}$  is defined as  $f_\theta(x) = \tilde{\alpha}^{(L)}(x)$ , where the activations and preactivations  $\alpha^{(\ell)}, \tilde{\alpha}^{(\ell)}$  are recursively constructed using the NTK parametrization: we set  $\alpha^{(0)}(x) = x$  and, for  $\ell = 0, \dots, L - 1$ ,

$$\tilde{\alpha}^{(\ell+1)}(x) = \frac{\sqrt{1 - \beta^2}}{\sqrt{n_\ell}} W^{(\ell)} \alpha^{(\ell)}(x) + \beta b^{(\ell)}, \quad \alpha^{(\ell+1)}(x) = \sigma\left(\tilde{\alpha}^{(\ell+1)}(x)\right),$$

where  $\sigma$  is applied entry-wise and  $\beta \geq 0$ .

*Remark 1.* The hyperparameter  $\beta$  allows one to balance the relative contributions of the connection weights and of the biases during training; in our numerical experiments, we set  $\beta = 0.1$ . Note that the variance of the normalized bias  $\beta b^{(\ell)}$  at initialization can be tuned by  $\beta$ .

### 2.1 Neural Tangent Kernel

The NTK [11] describes the evolution of  $(f_{\theta_t})_{t \geq 0}$  in function space during training. In the FC-NN case, the NTK  $\Theta_\theta^{(L)} : \mathbb{R}^{n_0} \times \mathbb{R}^{n_0} \rightarrow \mathbb{R}^{n_L \times n_L}$  is defined by

$$\Theta_{\theta, k k'}^{(L)}(x, x') = \sum_{p=1}^P \partial_{\theta_p} f_{\theta, k}(x) \partial_{\theta_p} f_{\theta, k'}(x').$$

For a dataset  $x_1, \dots, x_N \in \mathbb{R}^{n_0}$ , we define the *output* vector  $Y_\theta = (f_{\theta, k}(x_i))_{i, k} \in \mathbb{R}^{N n_L}$ . The DNN is trained by optimizing a cost  $C : \mathbb{R}^{n_L N} \rightarrow \mathbb{R}$  through gradient descent, defining a flow

$\partial_t \theta_t = -\nabla_{\theta} C(Y_{\theta})|_{\theta_t}$ . The evolution of the output vector  $Y_{\theta}$  can be expressed in terms of the NTK Gram Matrix  $\tilde{\Theta}_{\theta}^{(L)} = \left( \Theta_{\theta, km}^{(L)}(x_i, x_j) \right)_{ik, jm} \in \mathbb{R}^{n_L N \times n_L N}$  and gradient  $\nabla_Y C(Y_{\theta_t}) \in \mathbb{R}^{n_L N}$ :

$$\partial_t Y_{\theta_t} = -\tilde{\Theta}_{\theta}^{(L)} \nabla_Y C(Y_{\theta_t}).$$

## 2.2 Infinite-Width Limit

Following [18, 5, 16], in the overparametrized regime at initialization, the preactivations  $(\tilde{\alpha}_i^{(\ell)})_{i=1, \dots, n_{\ell}}$  are described by iid centered Gaussian processes with covariance kernels  $\Sigma^{(\ell)}$  constructed as follows. For a kernel  $K$ , set

$$\mathbb{L}_K^g(z_0, z_1) = \mathbb{E}_{(y_0, y_1) \sim \mathcal{N}(0, (K(z_i, z_j))_{i, j=0, 1})} [g(y_0) g(y_1)].$$

The activation kernels  $\Sigma^{(\ell)}$  are defined recursively by  $\Sigma^{(0)}(z_0, z_1) = \beta^2 + \frac{(1-\beta^2)}{n_0} z_0^T z_1$  and  $\Sigma^{(\ell+1)} = \beta^2 + (1-\beta^2) \mathbb{L}_{\Sigma^{(\ell)}}^{\sigma}$ .

While random at initialization, in the infinite-width-limit, the NTK converges to a deterministic limit, which is moreover constant during training:

**Theorem 2.** *As  $n_1, \dots, n_{L-1} \rightarrow \infty$ , for any  $z_0, z_1 \in \mathbb{R}^{n_0}$  and any  $t \geq 0$ , the kernel  $\Theta_{\theta_t}^{(L)}(z_0, z_1)$  converges to  $\Theta_{\infty}^{(L)}(z_0, z_1) \otimes \text{Id}_{n_L}$ , where  $\Theta_{\infty}^{(L)}(z_0, z_1) = \sum_{\ell=1}^L \Sigma^{(\ell)}(z_0, z_1) \prod_{l=\ell+1}^L \dot{\Sigma}^{(l)}(z_0, z_1)$  and  $\dot{\Sigma}^{(l)} = (1-\beta^2) \mathbb{L}_{\Sigma^{(l-1)}}^{\dot{\sigma}}$  with  $\dot{\sigma}$  denoting the derivative of  $\sigma$ .*

We refer to [11] for a proof for the sequential limit  $n_1 \rightarrow \infty, \dots, n_{L-1} \rightarrow \infty$  and [26, 2] for the simultaneous limit  $\min(n_1, \dots, n_{L-1}) \rightarrow \infty$ . As a consequence, in the infinite-width limit, the dynamics of the labels  $Y_{\theta_t, k} \in \mathbb{R}^N$  for each outputs  $k$  acquires a simple form in terms of the limiting NTK Gram matrix  $\tilde{\Theta}_{\infty}^{(L)} \in \mathbb{R}^{N \times N}$

$$\partial_t Y_{\theta_t, k} = -\tilde{\Theta}_{\infty}^{(L)} \nabla_{Y_k} C(Y_{\theta_t}).$$

## 3 Large Depth Limit

We now investigate the large  $L$  behavior on the NTK (in the infinite-width limit), revealing a transition between two phases: ‘‘order’’ and ‘‘chaos’’. To ensure that the variance of the neurons is constant for all depths ( $\Sigma^{(\ell)}(x, x) = 1$ ) we consider *standardized* nonlinearity  $\sigma$  (i.e. such that  $\mathbb{E}_{x \sim \mathcal{N}(0, 1)} [\sigma^2(x)] = 1$ ) and inputs on the *standard  $\sqrt{n_0}$ -sphere*<sup>1</sup>  $\mathbb{S}_{n_0} = \{x \in \mathbb{R}^{n_0} : \|x\| = \sqrt{n_0}\}$ .

### 3.1 Order and Chaos

For a standardized  $\sigma$ , the large-depth behavior of the *normalized NTK*  $\vartheta^{(L)}(x, y) = \Theta_{\infty}^{(L)}(x, y) / \sqrt{\Theta_{\infty}^{(L)}(x, x) \Theta_{\infty}^{(L)}(y, y)}$  is determined by the *characteristic value*

$$r_{\sigma, \beta} = (1 - \beta^2) \mathbb{E}_{x \sim \mathcal{N}(0, 1)} [\dot{\sigma}^2(x)]. \quad (3.1)$$

**Theorem 3.** *Suppose that  $\sigma$  is twice differentiable and standardized.*

**Order:** *If  $r_{\sigma, \beta} < 1$ , there exists  $C_1$  such that for  $x, y \in \mathbb{S}_{n_0}$ ,*

$$1 - C_1 L r_{\sigma, \beta}^L \leq \vartheta^{(L)}(x, y) \leq 1.$$

**Chaos:** *If  $r_{\sigma, \beta} > 1$ , for  $x \neq \pm y$  in  $\mathbb{S}_{n_0}$ , there exist  $h < 1$  and  $C_2$ , such that*

$$\left| \vartheta^{(L)}(x, y) \right| \leq C_2 h^L.$$

<sup>1</sup>Note that high dimensional datasets tend to concentrate on hyperspheres: for example in GANs [9] the inputs of a generator are vectors of iid  $\mathcal{N}(0, 1)$  entries which concentrate around  $\mathbb{S}_{n_0}$  for large dimensions.

Theorem 3 shows that in the ordered regime, the normalized NTK  $\vartheta^{(L)}$  converges to a constant as  $L \rightarrow \infty$ , whereas in the chaotic regime, it converges to a Kronecker  $\delta$  (taking value 1 on the diagonal, 0 elsewhere). This suggests that the training of deep FC-NN is heavily influenced by the characteristic value: when  $r_{\sigma,\beta} < 1$ ,  $\Theta^{(L)}$  becomes constant, thus slowing down the training, whereas when  $r_{\sigma,\beta} > 1$ ,  $\Theta^{(L)}$  is concentrated on the diagonal, ensuring fast training, but limiting generalization. To train very deep FC-NNs, it is necessary to lie ‘‘on the edge of chaos’’  $r_{\sigma,\beta} = 1$  [21, 28].

Theorem 3 does not apply directly to the standardized ReLU  $\sigma(x) = \sqrt{2} \max(x, 0)$ , because it is not differentiable in 0. The characteristic value for the standardized ReLU is  $r_{\sigma,\beta} = 1 - \beta^2$  which lies in the ordered regime for  $\beta > 0$

**Theorem 4.** *With the same notation as in Theorem 3, taking  $\sigma$  to be the standardized ReLU and  $\beta > 0$ , the NTK is in the ordered regime: there exists a constant  $C$  such that  $1 - Cr_{\sigma,\beta}^{L/2} \leq \vartheta^{(L)}(x, y) \leq 1$ .*

We observe two interesting (and potentially beneficial) properties of the standardized ReLU:

1. Its characteristic value  $r_{\sigma,\beta} = 1 - \beta^2$  is very close to the ‘edge of chaos’ for small  $\beta$  and typically with LeCun initialization the variance of the bias at initialization is  $1/w$  for  $w$  the width, which roughly corresponds to a choice of  $\beta = 1/\sqrt{w}$ .
2. The rate of convergence to the limiting kernel is smaller ( $r_{\sigma,\beta}^{L/2}$ ) for the ReLU than for differentiable nonlinearities ( $(r_{\sigma,\beta}^L)^2$ ).

These observations suggest that an advantage of the ReLU is that the NTK of ReLU networks converges to its constant limit at a slower rate and may naturally offer a good tradeoff between generalization and training speed.

### 3.2 Chaotic effect of normalization

Figure 3.1 shows that even on the edge of chaos, the NTK may exhibit a strong constant component (i.e.  $\vartheta(x, y) > 0.2$  for all  $x, y$ ) which can lead to a bad conditioning of the Gram matrix governing the infinite-width training behavior. It may be helpful to slightly ‘move’ the network towards the chaotic regime to reduce this effect. In Figure 3.1,  $r_{\sigma,\beta}$  plays a similar role to that of the lengthscale parameter in classical kernel methods: increasing  $r_{\sigma,\beta}$  makes the NTK ‘narrower’, reducing the correlation length.

From the definition 3.1 of the characteristic value, we see that increasing the bias pushes the network towards the ordered regime, whereas  $r_{\sigma,\beta}$  reaches its highest value  $\mathbb{E}[\dot{\sigma}^2(x)]$  when the bias is 0, which may still be in the ordered regime (or on the edge with the ReLU). We are therefore interested in ways to push the network further towards the chaotic regime.

In this section, we show that Layer Normalization is asymptotically equivalent to Nonlinearity Normalization which entails  $r_{\sigma,\beta} > 1$  for  $\beta$  small enough. While Batch normalization cannot be directly interpreted in terms of  $r_{\sigma,\beta}$ , it is easy to show that it directly controls the constant component of the NTK, which is characteristic of the ordered regime.

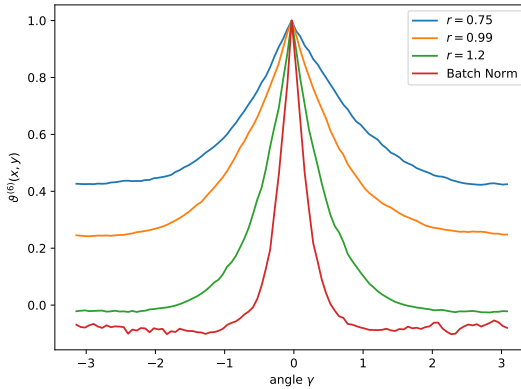


Figure 3.1: The NTK on the unit circle for four architectures with depth  $L = 6$  are plotted: vanilla ReLU network with  $\beta = 0.5$  (order) and  $\beta = 0.1$  (edge of chaos), with a normalized ReLU / Layer norm. (chaos) and with Batch Norm.

<sup>2</sup>Of course the rates of Theorems 3 and 4 may not be tight, but from the proofs in Appendix B.1 one can observe that the rate of  $r_{\sigma,\beta}^{L/2}$  appears as a result of the non-differentiability of the ReLU.

### 3.2.1 Nonlinearity Normalization and Layer Normalization

Intuitively, the dominating constant component in ReLU networks is partly a consequence of the ReLU being non-negative: after the first hidden layer, all negative correlations become positive (i.e.  $\Sigma^{(1)}(x, y) \geq \beta$  for all  $x, y$ , even  $x = -y$ ). One can address this issue thanks to the following. We shall write  $Z$  for a random variable with standard normal distribution. We say that  $\sigma$  is normalized if  $\mathbb{E}[\sigma(Z)] = 0$  and  $\mathbb{E}[\sigma(Z)^2] = 1$ . In particular, if  $\sigma \neq \text{id}$ , then  $\bar{\sigma}(\cdot) := \frac{\sigma(\cdot) - \mathbb{E}[\sigma(Z)]}{\sqrt{\mathbb{E}[(\sigma(Z) - \mathbb{E}[\sigma(Z)])^2]}}$  is normalized. By Poincaré Inequality, after nonlinearity normalization, one can always reach the chaotic regime:

**Proposition 5.** *If  $\sigma \neq \text{id}$  is normalized, then  $\mathbb{E}[\dot{\sigma}^2(Z)] > 1$  and  $r_{\sigma, \beta} > 1$  for  $\beta > 0$  small enough.*

With post-nonlinearity layer normalization, for every input  $x \in \mathbb{R}^{n_0}$  and every  $\ell = 1, \dots, L - 1$ , the activations become

$$\check{\alpha}^{(\ell)}(x) = \text{LN}(\alpha^{(\ell)}(x)) = \sqrt{n_\ell} \frac{\alpha^{(\ell)}(x) - \underline{\mu}^{(\ell)}(x)}{\|\alpha^{(\ell)}(x) - \underline{\mu}^{(\ell)}(x)\|},$$

where  $\underline{\mu}^{(\ell)}(x) = \frac{1}{n_\ell} \sum_{i=1}^{n_\ell} \alpha_i^{(\ell)}(x) (1 \cdots 1)^T$ . We define similarly pre-nonlinearity layer normalization with  $\check{\tilde{\alpha}}^{(\ell)}(x) = \sigma(\text{LN}(\check{\tilde{\alpha}}^{(\ell)}(x)))$ .

**Proposition 6.** *Suppose that the inputs belong to  $\mathbb{S}_{n_0}$ . Asymptotically, as the widths of the network sequentially go to infinity, post-nonlinearity layer normalization is equivalent to nonlinearity normalization, whereas pre-nonlinearity layer normalization has no effect.*

### 3.2.2 Batch Normalization

For any  $N \times d$  matrix of features  $X$  leading to a  $N \times N$  Gram matrix  $K = \frac{1}{d} X X^T$ , the Rayleigh quotient  $\frac{1}{N} \mathbf{1}^T K \mathbf{1}$  of the constant vector  $\mathbf{1}$  measures how big the constant component is. Applying Batch Normalization (BN) at a layer  $\ell$  centers (and standardizes) the activations<sup>3</sup>  $\alpha_j^{(\ell)}(x_i)$  over a batch  $x_1, \dots, x_N$ , thus zeroing the constant Rayleigh quotient of the  $N \times N$  features Gram matrices  $\tilde{\Sigma}^{(\ell)}$  with entries  $\tilde{\Sigma}_{ij}^{(\ell)} = \frac{1}{n_\ell} \sum_{k=1}^{n_\ell} \alpha_k^{(\ell)}(x_i) \alpha_k^{(\ell)}(x_j)$ . Adding a single BN layer after the last hidden layer controls the constant Rayleigh quotient of the NTK Gram matrix  $\tilde{\Theta}^{(L)}$ :

**Lemma 7.** *Consider FC-NN with  $L$  layers, with a PN-BN after the last nonlinearity then  $\frac{1}{N} \mathbf{1}^T \tilde{\Theta}^{(L)} \mathbf{1} = \beta^2$ .*

In contrast, for a network in the extreme order, i.e. such that  $\Theta^{(L)}(x, y) \approx c$  for some constant  $c > 0$ , the constant Rayleigh quotient scales as  $\frac{1}{N} \mathbf{1}^T \tilde{\Theta}^{(L)} \mathbf{1} \approx cN$ . The analysis of BN presented in [?] is also closely related to this phenomenon.

## 4 Convolutional Networks and Generative Adversarial Networks

The order/chaos transition is even more interesting for convolutional networks, in particular in the context of Generative Adversarial Networks (GANs): a common problem in GAN training is the so-called ‘mode collapse’, where the generator converges to a constant function, hence generating a single image instead of a variety of images. This problem is closely related to the fact that the constant mode of the NTK Gram matrix dominates, and indeed the problem of mode collapse is most prominent in the ordered regime (Figure 4.1), while normalization techniques (leading to a chaotic network) mitigate this problem.

In this section, we use the NTK to explain the appearance of border and checkerboard artifacts in generated images. We show that the border artifacts issue can be solved by a change of parametrization and that the checkerboard artifacts occur in the ordered regime, and can hence be avoided by adding normalization and using layer-wise learning rates. With these changes we are able to train GANs on CelebA dataset without Batch Normalization.

<sup>3</sup>We consider here *post-nonlinearity* BN, it is common to normalize the pre-activations  $\check{\tilde{\alpha}}^{(\ell)}$  instead.

## 4.1 Graph-based Neural Networks (GB-NNs)

In FC-NNs, the neurons are indexed by their layer  $\ell$  and their channel  $i \in \{1, \dots, n_\ell\}$ , in convolutional networks each neuron furthermore has a location on the image (or on a downscaled image). The position  $p$  of a neuron determines its connections with the neurons of the previous and subsequent layers. Furthermore certain connections are shared, i.e. they evolve together. We abstract these concepts in the following manner:

For each layer  $\ell = 0, \dots, L$ , the neurons are indexed by a position  $p \in I_\ell$  and a channel  $i = 1, \dots, n_\ell$ . The sets of positions  $I_\ell$  can be any set, in particular any subset of  $\mathbb{Z}^D$ . Each position  $p \in I_{\ell+1}$  has a set of parents  $P(p) \subset I_\ell$  which are neurons of the previous layer connected to  $p$ . The connections from the parent  $(q, \ell)$  to the position  $(p, \ell + 1)$  are encoded in an  $n_\ell \times n_{\ell+1}$  weight matrix  $W^{(\ell, q \rightarrow p)}$ . Finally two connections  $q \rightarrow p$  and  $q' \rightarrow p'$  can be shared, setting the corresponding matrices to be equal  $W^{(\ell, q \rightarrow p)} = W^{(\ell, q' \rightarrow p')}$ .

The inputs of the network  $x$  are vectors in  $(\mathbb{R}^{n_0})^{I_0}$ , for example for colour images of width  $w$  and height  $h$ , we have  $n_0 = 3$  and  $I_0 = \{1, \dots, w\} \times \{1, \dots, h\} \subset \mathbb{Z}^2$ . The activations and preactivations  $\alpha^{(\ell)}, \tilde{\alpha}^{(\ell)} \in (\mathbb{R}^{n_\ell})^{I_\ell}$  are constructed recursively using the NTK parametrization: we set  $\alpha^{(0, p)}(x) = x^{(p)}$  and for  $\ell = 0, \dots, L - 1$  and any position  $p \in I_{\ell+1}$ ,

$$\tilde{\alpha}^{(\ell+1, p)}(x) = \beta b^{(\ell)} + \frac{\sqrt{1 - \beta^2}}{\sqrt{|P(p)| n_\ell}} \sum_{q \in P(p)} W^{(\ell, q \rightarrow p)} \alpha^{(\ell, q)}(x), \quad \alpha^{(\ell+1, p)}(x) = \sigma \left( \tilde{\alpha}^{(\ell+1, p)}(x) \right) \quad (4.1)$$

where  $\sigma$  is applied entry-wise,  $\beta \geq 0$  and  $|P(p)|$  is the cardinality of  $P(p)$ .

### 4.1.1 Deconvolutional networks

Deconvolutional networks (DC-NNs) in dimension  $D$  can be seen as a special case of GB-NNs. We first consider borderless DC-NNs, i.e. the set of positions are  $I_\ell = \mathbb{Z}^D$  for all layers  $\ell$ . Given window dimensions  $(w_1, \dots, w_D)$  and strides  $(s_1, \dots, s_D)$ , the set of parents of  $p \in I_{\ell+1}$  is the hyperrectangle  $P(p) = \{[p_1/s_1] + 1, \dots, [p_1/s_1] + w_1\} \times \dots \times \{[p_D/s_D] + 1, \dots, [p_D/s_D] + w_D\} \subset \mathbb{Z}^D$ . Two connections  $q \rightarrow p$  and  $q' \rightarrow p'$  are shared if  $s_d | p_d - p'_d$  and  $q_d - q'_d = \frac{p_d - p'_d}{s_d}$  for all  $d = 1, \dots, D$ . This definition can easily be extended to any other choices of position sets  $I_\ell \subset \mathbb{Z}^D$  (for example hyperrectangles) by considering  $P(p) \cap I_\ell$  in place of  $P(p)$  as parents of  $p$ .

### 4.1.2 Neural Tangent Kernel

As for FC-NNs, in the infinite width limit (when  $n_1, \dots, n_{L-1} \rightarrow \infty$ ) the preactivations  $\tilde{\alpha}_i^{(\ell, p)}(x)$  converge to Gaussian processes with covariance

$$\text{Cov} \left( \tilde{\alpha}_i^{(\ell+1, p)}(x), \tilde{\alpha}_j^{(\ell+1, q)}(y) \right) = \delta_{ij} \Sigma^{(\ell, pq)}(x, y).$$

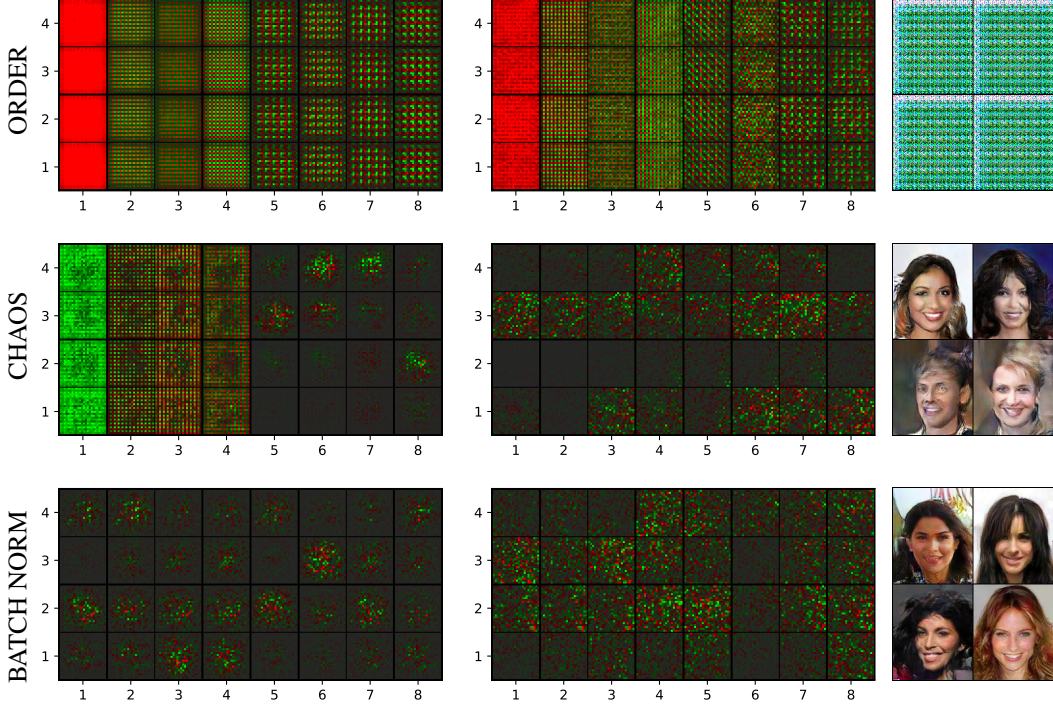
The behavior of the network during training is described by the NTK

$$\Theta_{ij}^{(\ell, pq)}(x, y) = \sum_{k=1}^P \partial_{\theta_k} \tilde{\alpha}_i^{(\ell+1, p)}(x) \partial_{\theta_k} \tilde{\alpha}_j^{(\ell+1, q)}(y).$$

In Section E of the Appendix we prove the convergence  $\Theta_{ij}^{(\ell, pq)}(x, y) \rightarrow \delta_{ij} \Theta_\infty^{(\ell, pq)}(x, y)$  of the NTK and give formulas for the limiting kernels  $\Sigma^{(\ell, pq)}(x, y)$  and  $\Theta_\infty^{(\ell, pq)}(x, y)$ .

### 4.1.3 Border Effects

A very important element of the NTK parametrization proposed in Section 4.1 is the factors  $1/\sqrt{|P(p)| n_\ell}$  in the definition of the preactivation (Equation 4.1): we scale the contribution of the previous layer according to the number of neurons  $|P(p)| n_\ell$  (i.e.  $n_\ell$  channels for each of the  $|P(p)|$  positions) which are fed into the neuron. For inputs  $x \in \mathbb{S}_{n_0}^{I_0}$  (i.e. such that  $x^{(p)} \in \mathbb{S}_{n_0}$  for all  $p$ ), these factors ensure that the limiting variance  $\Sigma^{(\ell, pp)}(x, x)$  of  $\tilde{\alpha}_i^{(\ell, p)}(x)$  at initialization is the same for all  $p$ :



standard                      graph-based + layer dependent lr.                      GAN

Figure 4.1: The left and middle columns represent the first 8 eigenvectors of the NTK Gram matrix of a DC-NN ( $L=3$ ) on 4 inputs. (left) without the Graph-Based Parametrization (GBP) and the Layer-Dependent Learning Rate (LDLR); (middle) with GBP and LDLR. The right column represents the results of a GAN on CelebA with GBP and LDLR. Each line correspond to a choice of nonlinearity/normalization for the generator: (top) ReLU, (middle) normalized ReLU and (bottom) ReLU with Batch Normalization.

**Proposition 8.** For GB-NNs with the NTK parametrization,  $\Sigma^{(\ell,pp)}(x, x)$  and  $\Theta_{\infty}^{(\ell,pp)}(x, x)$  do not depend neither on  $p \in I_{\ell}$  nor on  $x \in \mathbb{S}_{n_0}^{I_0}$ .

These factors are usually not present and to compensate, the variance of the weights at initialization is reduced. In convolutional networks with LeCun initialization, the standard deviation of the weights at initialization is set to  $\frac{1}{\sqrt{whn_{\ell}}}$  for  $w$  and  $h$  the width and height of the window of convolution, which has roughly the effect of replacing the  $\frac{1}{\sqrt{|P(p)|n_{\ell}}}$  factors by  $\frac{1}{\sqrt{whn_{\ell}}}$ . However  $whn_{\ell}$  is the maximal number of parents that a neuron can have, it is typically attained at positions  $p$  in the middle of the image. Positions  $p$  on the border of the image have less parents hence leading to a smaller contribution of the previous layer. This leads both kernels  $\Sigma^{(\ell,pp)}(x, x)$  and  $\Theta^{(\ell,pp)}(x, x)$  to have lower intensity for  $p \in I_{\ell}$  on the border (see Appendix G for an example when  $I_{\ell} = \mathbb{N}$ , i.e. when there is one border pixel), leading to border artifacts as seen in Figure 4.1.

## 4.2 Bulk Order and Chaos for Deconvolutional Nets

Large depths deconvolutional networks exhibit a similar Order/Chaos transition as that of FC-NNs, the values of the limiting kernel at different positions  $\Theta^{(L,pq)}$  is especially interesting.

For GB-NNs, the value of an output neuron at a position  $p \in I_L$  only depends on the inputs which are ancestors of  $p$ , i.e. all positions  $q \in I_0$  such that there is a chain of connections from  $q$  to  $p$ . For

the same reason, the NTK  $\Theta^{(L,pp')}(x, y)$  only depends on the values  $x_q, y_{q'}$  for  $q, q' \in I_0$  ancestors of  $p$  and  $p'$  respectively.

For a stride  $s \in \{2, 3, \dots\}^d$ , we denote the  $s$ -valuation  $v_s(n)$  of  $n \in \mathbb{Z}^d$  as the largest  $k \in \{0, 1, 2, \dots\}$  such that  $s_i^k \mid n_i$  for all  $i = 1, \dots, d$ . The behaviour of the NTK  $\Theta_{p,p'}^{(L)}(x, y)$  depends on the  $s$ -valuation of the difference of the two output positions. If  $v_s(p' - p)$  is strictly smaller than  $L$ , the NTK  $\Theta^{(L,pp')}(x, y)$  converges to a constant in the infinite-width limit for any  $x, y \in \mathbb{S}_{n_0}^{I_0}$ . Again the characteristic value  $r_{\sigma,\beta}$  plays a central role in the behavior of the large-depth limit. In this context, we define the rescaled NTK as  $\vartheta^{(L,pp')}(x, y) = \Theta^{(L,pp')}(x, y) / \sqrt{\Theta^{(L,pp)}(x, x)\Theta^{(L,pp')}(y, y)}$  (note that the denominator actually does not depend on  $p, p', x$  nor  $y$  by Proposition 8)

**Theorem 9.** *Consider a borderless DC-NN with position sets  $I_\ell = \mathbb{Z}^D$  for all layers  $\ell$ , upsampling stride  $s \in \{2, 3, \dots\}^D$  and window sizes  $w \in \{1, 2, 3, \dots\}^D$ . For a standardized twice differentiable  $\sigma$ , there exist constants  $C_1, C_2 > 0$ , such that the following holds: for  $x, y \in \mathbb{S}_{n_0}^{I_0}$ , and any positions  $p, p' \in I_L$ , we have*

**Order:** When  $r_{\sigma,\beta} < 1$ , taking  $v = \min(v_s(p - p'), L - 1)$ , we have

$$\frac{1 - r_{\sigma,\beta}^{v+1}}{1 - r_{\sigma,\beta}^L} - C_1(v + 1)r_{\sigma,\beta}^v \leq \vartheta^{(L,pp')}(x, y) \leq \frac{1 - r_{\sigma,\beta}^{v+1}}{1 - r_{\sigma,\beta}^L}.$$

**Chaos:** When  $r_{\sigma,\beta} > 1$ , if either  $v_s(p - p') < L$  or if there exists  $c < 1$  such that for all positions  $q \in I_0$  which are ancestors of  $p$ ,  $\left| x_q^T y_{q + \frac{p' - p}{sL}} \right| < c$ , then there exists  $h < 1$  such that

$$\left| \vartheta^{(L,pp')}(x, y) \right| \leq C_2 h^L.$$

This theorem suggests that in the order regime, the correlations between differing positions  $p$  and  $p'$  increase with  $v_s(p - p')$ , which is a strong feature of checkerboard patterns [19]. These artifacts typically appear in images generated by DC-NNs. The form of the NTK also suggests a strong affinity to these checkerboard patterns: they should dominate the NTK spectral decomposition. This is shown in Figure 4.1 where the eigenvectors of the NTK Gram matrix for a DC-NN are computed.

In the chaotic regime, the normalized NTK converges to a ‘‘scaled translation invariant’’ Kronecker delta. For two output positions  $p$  and  $p' = p + ks^L$  we associate the two regions  $\omega$  and  $\omega' = \omega + k$  of the input space which are connected to  $p$  and  $p'$ . Then  $\vartheta^{(L,p,p+ks^L)}(x, y)$  is one if the patch  $y_{\omega'}$  is a  $k$  translation of  $x_\omega$  and approximately zero otherwise.

#### 4.2.1 Layer-dependent learning rate

The NTK is the sum  $\Theta^{(L)} = \sum_\ell \Theta_{W^{(\ell)}}^{(L)} + \Theta_{b^{(\ell)}}^{(L)}$  over the contributions of the weights  $\Theta_{W^{(\ell)}}^{(L,pq)}(x, y) = \sum_{ij} \partial_{W_{ij}^{(\ell)}} f_{\theta,p}(x) \partial_{W_{ij}^{(\ell)}} f_{\theta,q}(y)$  and biases  $\Theta_{b^{(\ell)}}^{(L,pq)}(x, y) = \sum_j \partial_{b_j^{(\ell)}} f_{\theta,p}(x) \partial_{b_j^{(\ell)}} f_{\theta,q}(y)$ . At the  $\ell$ -th layer, the weights and biases can only contribute to checkerboard patterns of degree  $v = L - \ell$  and  $v = L - \ell - 1$ , i.e. patterns with periods  $s^{L-\ell}$  and  $s^{L-\ell-1}$  respectively, in the following sense:

**Proposition 10.** *In a DC-NN with stride  $s \in \{2, 3, \dots\}^d$ , we have  $\Theta_{\infty, W^{(\ell)}}^{(L,pp')}(x, y) = 0$  if  $s^{L-\ell} \nmid p' - p$  and  $\Theta_{\infty, b^{(\ell)}}^{(L,pp')}(x, y) = 0$  if  $s^{L-\ell-1} \nmid p' - p$ .*

This suggests that the supports of  $\Theta_{\infty, W^{(\ell)}}^{(L)}$  and  $\Theta_{\infty, b^{(\ell)}}^{(L)}$  increase exponentially with  $\ell$ , giving more importance to the last layers during training. This could explain why the checkerboard patterns of lower degree dominate in Figure 4.1. In the classical parametrization, the balance is restored by letting the number of channels  $n_\ell$  decrease with depth [22]. In the NTK parametrization, the limiting NTK is not affected by the ratios  $n_\ell/n_k$ . To achieve the same effect, we divide the learning rate of the weights and bias of the  $\ell$ -th layer by  $S^{\ell/2}$  and  $S^{(\ell+1)/2}$  respectively, where  $S = \prod_i s_i$  is the product of the strides. Together with the ‘parent-based’ parametrization and the normalization of the nonlinearity (in order to lie in the chaotic regime) this rescaling of the learning rate removes both border and checkerboard artifacts in Figure 4.1.



## 5 Conclusion

This article shows how the NTK can be used theoretically to understand the effect of architecture choices (such as decreasing the number of channels or batch normalization) on the training of DNNs. We have shown that DNNs in a “order” regime, have a strong affinity to constant modes and checkerboard artifacts: this slows down training and can contribute to a mode collapse of the DC-NN generator of GANs. We introduce simple modifications to solve these problems: the effectiveness of normalizing the nonlinearity, a parent-based parametrization and a layer-dependent learning rates is shown both theoretically and numerically.

## Broader Impact

This work is theoretical and has as such no direct social impact.

## References

- [1] Zeyuan Allen-Zhu, Yuanzhi Li, and Zhao Song. A Convergence Theory for Deep Learning via Over-Parameterization. *CoRR*, abs/1811.03962, 2018.
- [2] Sanjeev Arora, Simon S Du, Wei Hu, Zhiyuan Li, Ruslan Salakhutdinov, and Ruosong Wang. On exact computation with an infinitely wide neural net. *arXiv preprint arXiv:1904.11955*, 2019.
- [3] Devansh Arpit, Yingbo Zhou, Bhargava Kota, and Venu Govindaraju. Normalization propagation: A parametric technique for removing internal covariate shift in deep networks. In Maria Florina Balcan and Kilian Q. Weinberger, editors, *Proceedings of The 33rd International Conference on Machine Learning*, volume 48 of *Proceedings of Machine Learning Research*, pages 1168–1176, New York, New York, USA, 20–22 Jun 2016. PMLR.
- [4] Andrew Brock, Jeff Donahue, and Karen Simonyan. Large scale gan training for high fidelity natural image synthesis. *arXiv preprint arXiv:1809.11096*, 2018.
- [5] Youngmin Cho and Lawrence K. Saul. Kernel Methods for Deep Learning. In *Advances in Neural Information Processing Systems 22*, pages 342–350. Curran Associates, Inc., 2009.
- [6] Amit Daniely, Roy Frostig, and Yoram Singer. Toward Deeper Understanding of Neural Networks: The Power of Initialization and a Dual View on Expressivity. In D. D. Lee, M. Sugiyama, U. V. Luxburg, I. Guyon, and R. Garnett, editors, *Advances in Neural Information Processing Systems 29*, pages 2253–2261. Curran Associates, Inc., 2016.
- [7] Simon S. Du, Xiyu Zhai, Barnabás Póczos, and Aarti Singh. Gradient Descent Provably Optimizes Over-parameterized Neural Networks. 2019.
- [8] Xavier Glorot and Yoshua Bengio. Understanding the difficulty of training deep feedforward neural networks. In *Proceedings of the Thirteenth International Conference on Artificial Intelligence and Statistics*, volume 9 of *Proceedings of Machine Learning Research*, pages 249–256, Chia Laguna Resort, Sardinia, Italy, 13–15 May 2010. PMLR.
- [9] Ian J. Goodfellow, Jean Pouget-Abadie, Mehdi Mirza, Bing Xu, David Warde-Farley, Sherjil Ozair, Aaron Courville, and Yoshua Bengio. Generative Adversarial Networks. *NIPS’14 Proceedings of the 27th International Conference on Neural Information Processing Systems - Volume 2*, pages 2672–2680, jun 2014.
- [10] Sergey Ioffe and Christian Szegedy. Batch normalization: Accelerating deep network training by reducing internal covariate shift. *CoRR*, abs/1502.03167, 2015.
- [11] Arthur Jacot, Franck Gabriel, and Clément Hongler. Neural Tangent Kernel: Convergence and Generalization in Neural Networks. In *Advances in Neural Information Processing Systems 31*, pages 8580–8589. Curran Associates, Inc., 2018.
- [12] Ryo Karakida, Shotaro Akaho, and Shun-Ichi Amari. Universal Statistics of Fisher Information in Deep Neural Networks: Mean Field Approach. jun 2018.

- [13] Tero Karras, Samuli Laine, and Timo Aila. A style-based generator architecture for generative adversarial networks. *arXiv preprint arXiv:1812.04948*, 2018.
- [14] Günter Klambauer, Thomas Unterthiner, Andreas Mayr, and Sepp Hochreiter. Self-normalizing neural networks. In I. Guyon, U. V. Luxburg, S. Bengio, H. Wallach, R. Fergus, S. Vishwanathan, and R. Garnett, editors, *Advances in Neural Information Processing Systems 30*, pages 971–980. Curran Associates, Inc., 2017.
- [15] Yann A LeCun, Léon Bottou, Genevieve B Orr, and Klaus-Robert Müller. Efficient backprop. In *Neural networks: Tricks of the trade*, pages 9–48. Springer, 2012.
- [16] Jae Hoon Lee, Yasaman Bahri, Roman Novak, Samuel S. Schoenholz, Jeffrey Pennington, and Jascha Sohl-Dickstein. Deep Neural Networks as Gaussian Processes. *ICLR*, 2018.
- [17] J. Lei Ba, J. R. Kiros, and G. E. Hinton. Layer Normalization. *arXiv e-prints*, July 2016.
- [18] Radford M. Neal. *Bayesian Learning for Neural Networks*. Springer-Verlag New York, Inc., Secaucus, NJ, USA, 1996.
- [19] Augustus Odena, Vincent Dumoulin, and Chris Olah. Deconvolution and checkerboard artifacts. *Distill*, 1(10):e3, 2016.
- [20] Daniel S Park, Samuel L Smith, Jascha Sohl-dickstein, and Quoc V Le. Optimal SGD Hyperparameters for Fully Connected Networks. 2018.
- [21] Ben Poole, Subhaneil Lahiri, Maithra Raghu, Jascha Sohl-Dickstein, and Surya Ganguli. Exponential expressivity in deep neural networks through transient chaos. In D. D. Lee, M. Sugiyama, U. V. Luxburg, I. Guyon, and R. Garnett, editors, *Advances in Neural Information Processing Systems 29*, pages 3360–3368. Curran Associates, Inc., 2016.
- [22] Alec Radford, Luke Metz, and Soumith Chintala. Unsupervised representation learning with deep convolutional generative adversarial networks. *arXiv preprint arXiv:1511.06434*, 2015.
- [23] Tim Salimans and Durk P Kingma. Weight normalization: A simple reparameterization to accelerate training of deep neural networks. In D. D. Lee, M. Sugiyama, U. V. Luxburg, I. Guyon, and R. Garnett, editors, *Advances in Neural Information Processing Systems 29*, pages 901–909. Curran Associates, Inc., 2016.
- [24] Shibani Santurkar, Dimitris Tsipras, Andrew Ilyas, and Aleksander Madry. How does batch normalization help optimization? In S. Bengio, H. Wallach, H. Larochelle, K. Grauman, N. Cesa-Bianchi, and R. Garnett, editors, *Advances in Neural Information Processing Systems 31*, pages 2483–2493. Curran Associates, Inc., 2018.
- [25] Sitao Xiang and Hao Li. On the effects of batch and weight normalization in generative adversarial networks. *arXiv preprint arXiv:1704.03971*, 2017.
- [26] Greg Yang. Scaling Limits of Wide Neural Networks with Weight Sharing: Gaussian Process Behavior, Gradient Independence, and Neural Tangent Kernel Derivation. *arXiv e-prints*, page arXiv:1902.04760, Feb 2019.
- [27] Greg Yang, Jeffrey Pennington, Vinay Rao, Jascha Sohl-Dickstein, and Samuel S. Schoenholz. A mean field theory of batch normalization. *CoRR*, abs/1902.08129, 2019.
- [28] Greg Yang and Samuel Schoenholz. Mean field residual networks: On the edge of chaos. In I. Guyon, U. V. Luxburg, S. Bengio, H. Wallach, R. Fergus, S. Vishwanathan, and R. Garnett, editors, *Advances in Neural Information Processing Systems 30*, pages 7103–7114. Curran Associates, Inc., 2017.
- [29] Han Zhang, Ian Goodfellow, Dimitris Metaxas, and Augustus Odena. Self-attention generative adversarial networks. *arXiv preprint arXiv:1805.08318*, 2018.

## A Choice of Parametrization

The NTK parametrization introduced in Section 2 differs slightly from the one usually used, yet it ensures that the training is consistent as the size of the layers grows. In the standard parametrization, the activations are defined by

$$\begin{aligned}\alpha^{(0)}(x; \theta) &= x \\ \tilde{\alpha}^{(\ell+1)}(x; \theta) &= W^{(\ell)} \alpha^{(\ell)}(x; \theta) + b^{(\ell)} \\ \alpha^{(\ell+1)}(x; \theta) &= \sigma \left( \tilde{\alpha}^{(\ell+1)}(x; \theta) \right).\end{aligned}$$

Let denote by  $g_\theta$  the output function of the DNN thus parametrized, and  $f_\theta$  that of the DNN with NTK parametrization. Note the absence of  $1/\sqrt{n_\ell}$  in comparison to the NTK parametrization. With LeCun/He initialization [15], the parameters  $W^{(\ell)}$  have standard deviation  $1/\sqrt{n_\ell}$  (or  $\sqrt{2}/\sqrt{n_\ell}$  for the ReLU but this does not change the general analysis). Using this initialization, the activations stay stochastically bounded as the widths of the DNN get large. In the forward pass, there is almost no difference between the two parametrizations and for each choice of parameters  $\theta$ , we can scale down the connection weights by  $\sqrt{1-\beta^2}/\sqrt{n_\ell}$  and the bias weights by  $\beta$  to obtain a new set of parameters  $\hat{\theta}$  such that

$$f_\theta = g_{\hat{\theta}}.$$

The two parametrizations will exhibit a difference during backpropagation since:

$$\partial_{W_{ij}^{(\ell)}} g_{\hat{\theta}}(x) = \frac{\sqrt{n_\ell}}{\sqrt{1-\beta^2}} \partial_{W_{ij}^{(\ell)}} f_\theta(x), \quad \partial_{b_j^{(\ell)}} g_{\hat{\theta}}(x) = \frac{1}{\beta} \partial_{b_j^{(\ell)}} f_\theta(x).$$

The NTK is a sum of products of these derivatives over all parameters:

$$\Theta^{(L)} = \Theta^{(L:W^{(0)})} + \Theta^{(L:b^{(0)})} + \Theta^{(L:W^{(1)})} + \Theta^{(L:b^{(1)})} + \dots + \Theta^{(L:W^{(L-1)})} + \Theta^{(L:b^{(L-1)})}.$$

With our parametrization, all summands converge to a finite limit, while with the Le Cun or He parameterization we obtain

$$\hat{\Theta}^{(L)} = \frac{n_0}{1-\beta^2} \Theta^{(L:W^{(0)})} + \frac{1}{\beta^2} \Theta^{(L:b^{(0)})} + \dots + \frac{n_{L-1}}{1-\beta^2} \Theta^{(L:W^{(L-1)})} + \frac{1}{\beta^2} \Theta^{(L:b^{(L-1)})},$$

where some summands, namely the  $\left(\frac{n_i}{1-\beta^2} \Theta^{(L:W^{(i)})}\right)_i$ , explode in the infinite width limit. One must therefore take a learning rate of order  $1/\max(n_1, \dots, n_{L-1})$  [12, 20] to obtain a meaningful training dynamics, but in this case the contributions to the NTK of the first layers connections  $W^{(0)}$  and the bias of all layers  $b^{(\ell)}$  vanish, which implies that training these parameters has less and less effect on the function as the width of the network grows. As a result, the dynamics of the output function during training can still be described by a modified kernel gradient descent: the modified learning rate compensates for the absence of normalization in the usual parametrization.

The NTK parametrization is hence more natural for large networks, as it solves both the problem of having meaningful forward and backward passes, and to avoid tuning the learning rate, which is the problem that sparked multiple alternative initialization strategies in deep learning [8]. Note that in the standard parametrization, the importance of the bias parameters shrinks as the width gets large; this can be implemented in the NTK parametrization by taking a small value for the parameter  $\beta$ .

## B FC-NN Order and Chaos

In this section, we prove the existence of two regimes, ‘order’ and ‘chaos’, in FC-NNs. First, we improve some results of [6], and study the rate of convergence of the activation kernels as the depth grows to infinity. In a second step, this allows us to characterise the behavior of the NTK for large depth.

Let us consider a standardized differentiable nonlinearity  $\sigma$ , i.e. satisfying  $\mathbb{E}_{x \sim \mathcal{N}(0,1)} [\sigma^2(x)] = 1$ . Recall that the activation kernels are defined recursively by  $\Sigma^{(1)}(x, y) = \frac{1-\beta^2}{n_0} x^T y + \beta^2$  and  $\Sigma^{(\ell+1)}(x, y) = (1-\beta^2) \mathbb{L}_{\Sigma^{(\ell)}}^\sigma(x, y) + \beta^2$ , where  $\mathbb{L}_{\Sigma^{(\ell)}}^\sigma$  was introduced in Section 2.2. By induction,



Figure A.1: Result of two GANs on CelebA. (Left) with Nonlinearity Normalization and (Right) with Batch Normalization. In both cases the discriminator uses a Normalized ReLU.

for any  $x, y \in \mathbb{S}_{n_0}$ ,  $\Sigma^{(\ell+1)}(x, y)$  is uniquely determined by  $\rho_{x,y} = \frac{1}{n_0} x^T y$ . Defining the two functions  $R_\sigma, B_\beta : [-1, 1] \rightarrow [-1, 1]$  by:

$$R_\sigma(\rho) = \mathbb{E}_{v \sim \mathcal{N}\left(0, \begin{pmatrix} 1 & \rho \\ \rho & 1 \end{pmatrix}\right)} [\sigma(v_0)\sigma(v_1)],$$

$$B_\beta(\rho) = \beta^2 + (1 - \beta^2)\rho,$$

one can formulate the activation kernels as an alternate composition of  $B_\beta$  and  $R_\sigma$ :

$$\Sigma^{(\ell)}(x, y) = (B_\beta \circ R_\sigma)^{\circ \ell - 1} \circ B_\beta(\rho_{x,y}).$$

In particular, this shows that for any  $x, y \in \mathbb{S}_{n_0}$ ,  $\Sigma^{(\ell)}(x, y) \leq 1$ . Since the activation kernels are obtained by iterating the same function, we first study the fixed points of the composition  $B_\beta \circ R_\sigma : [-1, 1] \rightarrow [-1, 1]$ . When  $\sigma$  is a standardized nonlinearity, the function  $R_\sigma$ , named the dual of  $\sigma$ , satisfies the following key properties proven in [6]:

1.  $R_\sigma(1) = 1$ ,
2. For any  $\rho \in (-1, 0)$ ,  $R_\sigma(\rho) > \rho$ ,
3.  $R_\sigma$  is convex in  $[0, 1)$ ,
4.  $R'_\sigma(1) = \mathbb{E}[\dot{\sigma}(x)^2]$ , where  $R'_\sigma$  denotes the derivative of  $R_\sigma$ ,
5.  $R'_\sigma = R_{\dot{\sigma}}$ .

By definition  $B_\beta(1) = 1$ , thus 1 is a trivial fixed point:  $B_\beta \circ R_\sigma(1) = 1$ . This shows that for any  $x \in \mathbb{S}_{n_0}$  and any  $\ell \geq 1$ :

$$\Sigma^{(\ell)}(x, x) = 1.$$

It appears that  $-1$  is also a fixed point of  $B_\beta \circ R_\sigma$  if and only if the nonlinearity  $\sigma$  is antisymmetric and  $\beta = 0$ . From now on, we will focus on the region  $(-1, 1)$ . From the property 2. of  $R_\sigma$  and since  $B_\beta$  is non decreasing, any non trivial fixed point must lie in  $[0, 1)$ . Since  $B_\beta \circ R_\sigma(0) > 0$ ,  $B_\beta \circ R_\sigma(1) = 1$  and  $R_\sigma$  is convex in  $[0, 1)$ , there exists a non trivial fixed point of  $B_\beta \circ R_\sigma$  if  $(B_\beta \circ R_\sigma)'(1) > 1$  whereas if  $(B_\beta \circ R_\sigma)'(1) < 1$  there is no fixed point in  $(-1, 1)$ . This leads to two regimes shown in [6], depending on the value of  $r_{\sigma,\beta} = (1 - \beta^2) \mathbb{E}_{x \sim \mathcal{N}(0,1)}[\dot{\sigma}^2(x)]$ :

1. “Order” when  $r_{\sigma,\beta} < 1$ :  $B_\beta \circ R_\sigma$  has a unique fixed point equal to 1 and the activation kernels become constant at an exponential rate,

2. “Chaos” when  $r_{\sigma,\beta} > 1$ :  $B_\beta \circ R_\sigma$  has another fixed point  $0 \leq a < 1$  and the activation kernels converge to a kernel equal to 1 if  $x = y$  and to  $a$  if  $x \neq y$  and, if the nonlinearity is antisymmetric and  $\beta = 0$ , it converges to  $-1$  if and only if  $x = -y$ .

To establish the existence of the two regimes for the NTK, we need the following bounds on the rate of convergence of  $\Sigma^{(\ell)}(x, y)$  in the “order” region and on its values in the “chaos” region:

**Lemma 11.** *If  $\sigma$  is a standardized differentiable nonlinearity,*

*If  $r_{\sigma,\beta} < 1$ , then for any  $x, y \in \mathbb{S}_{n_0}$ ,*

$$1 \geq \Sigma^{(\ell)}(x, y) \geq 1 - 2r_{\sigma,\beta}^{\ell-1}(1 - \beta^2).$$

*If  $r_{\sigma,\beta} > 1$ , then there exists a fixed point  $a \in [0, 1)$  of  $B_\beta \circ R_\sigma$  such that for any  $x, y \in \mathbb{S}_{n_0}$ ,*

$$\left| \Sigma^{(\ell)}(x, y) \right| \leq \max \left\{ \left| \beta^2 + \frac{1 - \beta^2}{n_0} x^T y \right|, a \right\}.$$

*Proof.* Let us denote  $r = r_{\sigma,\beta}$  and suppose first that  $r < 1$ . By [6], we know that  $R'_\sigma = R_{\dot{\sigma}}$  and  $R_{\dot{\sigma}}(\rho) \in [-\mathbb{E}[\dot{\sigma}(z)^2], \mathbb{E}[\dot{\sigma}(z)^2]]$  where  $z \sim \mathcal{N}(0, 1)$ . From now on, we will omit to specify the distribution assumption on  $z$ . The previous equalities and inequalities imply that  $R_\sigma(\rho) \geq 1 - \mathbb{E}[\dot{\sigma}(v)^2](1 - \rho)$ , thus we obtain:

$$\begin{aligned} B_\beta \circ R_\sigma(\rho) &\geq \beta^2 + (1 - \beta^2)(1 - \mathbb{E}[\dot{\sigma}(z)^2](1 - \rho)) \\ &= 1 - (1 - \beta^2)\mathbb{E}[\dot{\sigma}(z)^2](1 - \rho) \\ &= 1 - r(1 - \rho). \end{aligned}$$

By definition, we then have  $\Sigma^{(\ell)}(x, y) = (B_\beta \circ R_\sigma)^{\circ \ell-1} \circ B_\beta \left( \frac{1}{n_0} x^T y \right) \geq 1 - 2(1 - \beta^2)r^{\ell-1}$ .

Using the bound  $\Sigma^{(\ell)}(x, y) \leq 1$ , this proves the first assertion.

When  $r > 1$ , there exists a fixed point  $a$  of  $B_\beta \circ R_\sigma$  in  $[0, 1)$ . By a convexity argument, for any  $\rho$  in  $[a, 1)$ ,  $a \leq B_\beta \circ R_\sigma(\rho) \leq \rho$  and because  $R_\sigma(\rho)$  is increasing in  $[0, 1)$ , for all  $\rho \in [0, a]$ ,  $0 \leq B_\beta \circ R_\sigma(\rho) \leq a$ .

For negative  $\rho$ , we claim that  $|B_\beta \circ R_\sigma(\rho)| \leq B_\beta \circ R_\sigma(|\rho|)$ , which entails the second assertion. Since  $R_\sigma(\rho) = \sum_{i=0}^{\infty} b_i \rho^i$  for positive  $b_i$ s [6], and the composition  $B_\beta \circ R_\sigma(\rho) = \sum_{i=0}^{\infty} c_i \rho^i$  for  $c_0 = b_0(1 - \beta^2) + \beta^2 \geq 0$  and  $c_i = b_i(1 - \beta^2) \geq 0$  when  $i > 0$ , we have

$$|B_\beta \circ R_\sigma(\rho)| = \left| \sum_{i=0}^{\infty} c_i \rho^i \right| \leq \sum_{i=0}^{\infty} c_i |\rho|^i = B_\beta \circ R_\sigma(|\rho|).$$

This leads to the inequality in the chaos regime.  $\square$

Before studying the normalized NTK, let us remark that the NTK on the diagonal (with  $x = y$  in  $\mathbb{S}_{n_0}$ ) is equal to:

$$\begin{aligned} \Theta_\infty^{(L)}(x, x) &= \sum_{\ell=1}^L \Sigma^{(\ell)}(x, x) \prod_{k=\ell+1}^L \dot{\Sigma}^{(k)}(x, x) \\ &= \sum_{\ell=1}^L \left( (1 - \beta^2) \mathbb{E}[\dot{\sigma}(x)^2] \right)^{L-\ell} \\ &= \frac{1 - r^L}{1 - r}. \end{aligned}$$

This shows that in the “order” regime,  $\Theta_\infty^{(L)}(x, x) \xrightarrow{L \rightarrow \infty} 1/(1-r)$  and in the “chaos” regime  $\Theta_\infty^{(L)}(x, x)$  grows exponentially. At the transition,  $r = 1$  and thus  $\Theta_\infty^{(L)}(x, x) = L$ . Besides, if  $x, y \in \mathbb{S}_{n_0}$ , using the Cauchy-Schwarz inequality, for any  $\ell$ ,  $|\Sigma^{(\ell)}(x, y)| \leq |\Sigma^{(\ell)}(x, x)|$  and  $\left| \dot{\Sigma}^{(\ell+1)}(x, y) \right| \leq \left| \dot{\Sigma}^{(\ell+1)}(x, x) \right|$ . This implies the following inequality:  $\Theta_\infty^{(L)}(x, y) \leq \Theta_\infty^{(L)}(x, x)$ .

We now study the normalized NTK  $\vartheta_L(x, y) = \frac{\Theta_\infty^{(L)}(x, y)}{\Theta_\infty^{(L)}(x, x)} \leq 1$ .

**Theorem 12.** *Suppose that  $\sigma$  is twice differentiable and standardized.*

*If  $r < 1$ , we are in the ordered regime: there exists  $C_1$  such that for  $x, y \in \mathbb{S}_{n_0}$ ,*

$$1 - C_1 L r^L \leq \vartheta^{(L)}(x, y) \leq 1.$$

*If  $r > 1$ , we are in the chaotic regime: for  $x \neq y$  in  $\mathbb{S}_{n_0}$ , there exist  $s < 1$  and  $C_2$ , such that*

$$\left| \vartheta^{(L)}(x, y) \right| \leq C_2 s^L.$$

*Proof.* First, let us suppose that  $r < 1$ . Recall that the NTK is defined as

$$\Theta_\infty^{(L)}(x, y) = \sum_{\ell=1}^L \Sigma^{(\ell)}(x, y) \dot{\Sigma}^{(\ell+1)}(x, y) \dots \dot{\Sigma}^{(L)}(x, y).$$

For all  $\ell$ ,  $\Sigma^{(\ell)}(x, y) \leq \Sigma^{(\ell)}(x, x) = 1$  and  $\dot{\Sigma}^{(\ell)}(x, y) \leq \dot{\Sigma}^{(\ell)}(x, x) = r$ . Writing  $\Sigma^{(\ell)}(x, y) = 1 - \epsilon^{(\ell)}$  and  $\dot{\Sigma}^{(\ell)}(x, y) = r - \dot{\epsilon}^{(\ell)}$  for  $\epsilon^{(\ell)}, \dot{\epsilon}^{(\ell)} \geq 0$  we have

$$\begin{aligned} \Theta_\infty^{(L)}(x, y) &= \sum_{\ell=1}^L \left(1 - \epsilon^{(\ell)}\right) \prod_{k=\ell+1}^L r - \dot{\epsilon}^{(\ell)} \\ &\leq \sum_{\ell=1}^L r^{L-\ell} - r^{L-\ell} \epsilon^{(\ell)} - \sum_{k=\ell+1}^L r^{L-\ell-1} \dot{\epsilon}^{(\ell)} \end{aligned}$$

Using the bound of Lemma 11 and the fact that for any  $x, y \in \mathbb{S}_{n_0}$ ,  $\dot{\Sigma}^{(\ell)}(x, y) = (1 - \beta^2) R_{\dot{\sigma}}(\Sigma^{(\ell-1)}(x, y)) \geq r - \psi \epsilon^{(\ell-1)}$  for  $\psi = (1 - \beta^2) \mathbb{E}_{z \sim \mathcal{N}(0,1)} [\dot{\sigma}(z)]$ , we obtain  $\epsilon^{(\ell)} < 2(1 - \beta^2) r^{\ell-1}$  and  $\dot{\epsilon}^{(\ell)} \leq 2(1 - \beta^2) \psi r^{\ell-2}$ . As a result:

$$\begin{aligned} \Theta_\infty^{(L)}(x, y) &\geq \sum_{\ell=1}^L r^{L-\ell} - 2(1 - \beta^2) r^{L-\ell} r^{\ell-1} - \sum_{k=\ell+1}^L 2(1 - \beta^2) \psi r^{L-\ell-1} r^{k-2} \\ &= \Theta_\infty^{(L)}(x, x) - 2(1 - \beta^2) \sum_{\ell=1}^L r^{L-1} + \psi \sum_{k=\ell+1}^L r^{L-\ell+k-3} \\ &= \Theta_\infty^{(L)}(x, x) - 2(1 - \beta^2) \left[ L r^{L-1} + \psi \sum_{\ell=1}^L \sum_{k=0}^{L-\ell-1} r^{L+k-2} \right] \\ &= \Theta_\infty^{(L)}(x, x) - 2(1 - \beta^2) \left[ L r^{L-1} + \psi r^{L-2} \sum_{\ell=1}^L \frac{1 - r^{L-\ell}}{1 - r} \right] \\ &\geq \Theta_\infty^{(L)}(x, x) - 2(1 - \beta^2) \left[ r + \psi \frac{1}{1 - r} \right] L r^{L-2} \\ &\geq \Theta_\infty^{(L)}(x, x) - C L r^L. \end{aligned}$$

Now, let us suppose that  $r > 1$ . Recall that  $B_\beta \circ R_\sigma$  has a unique fixed point  $a$  on  $[0, 1]$ . For any  $x$  and  $y$  in  $\mathbb{S}_{n_0}$ , the kernels  $\Sigma^{(\ell)}(x, y)$  are bounded in norm by  $v = \max \left\{ \left| \beta^2 + \frac{1-\beta^2}{n_0} x^T y \right|, a \right\}$  from Lemma 11. For the kernels  $\dot{\Sigma}^{(\ell)}$  we have  $\left| \dot{\Sigma}^{(\ell)}(x, y) \right| = (1 - \beta^2) \left| R_{\dot{\sigma}}(\Sigma^{(\ell-1)}(x, y)) \right| \leq (1 - \beta^2) R_{\dot{\sigma}}(|\Sigma^{(\ell-1)}(x, y)|) \leq (1 - \beta^2) R_{\dot{\sigma}}(v) =: w$  where the first inequality follows from the fact that  $R_{\dot{\sigma}}(\rho) = \sum_i b_i \rho^i$  for  $b_i \geq 0$  and the second follows from the monotonicity of  $R_{\dot{\sigma}}$  in  $[0, 1]$ . Applying these two bounds, we obtain:

$$\left| \Theta_\infty^{(L)}(x, y) \right| \leq \sum_{\ell=1}^L v \prod_{k=\ell+1}^L w = v \frac{1 - w^L}{1 - w}.$$

Since  $\Theta_\infty^{(L)}(x, y) = \frac{1-r^L}{1-r}$ , we have that  $|\vartheta_L(x, y)| \leq v \frac{1-w^L}{1-r}$ . If  $x \neq y$  then  $v < 1$  and since  $\sigma$  is nonlinear,  $w = (1 - \beta^2) R_{\dot{\sigma}}(v) < (1 - \beta^2) R_{\dot{\sigma}}(1) = r$ . This implies that  $|\vartheta_L(x, y)|$  converges to zero at an exponential rate, as  $L \rightarrow \infty$ .  $\square$

## B.1 ReLU FC-NN

For the standardized ReLU nonlinearity,  $\sigma(x) = \sqrt{2} \max(x, 0)$ , the dual activation is computed in [6]:

$$R_\sigma(\rho) = \frac{\sqrt{1-\rho^2} + (\pi - \cos^{-1}(\rho))\rho}{\pi},$$

and the dual activation of its derivative is given by:

$$R_{\dot{\sigma}}(\rho) = \frac{\pi - \cos^{-1}(\rho)}{\pi}.$$

The characteristic value  $r = r_{\sigma, \beta}$  of the standardized ReLU is equal to  $1 - \beta^2$ : the ReLU nonlinearity therefore lies in the ‘‘order’’ regime as soon as  $\beta > 0$ . More explicitly, Lemma 11 still holds of the standardized ReLU and, using the value of  $r$ , the following inequalities hold for any  $x, y \in \mathbb{S}_{n_0}$ :

$$1 \geq \Sigma^{(\ell)}(x, y) \geq 1 - 2r^\ell.$$

Using these bounds, we can now prove Theorem 13.

**Theorem 13.** *With the same notation as in Theorem 12, taking  $\sigma$  to be the standardized ReLU and  $\beta > 0$ , we are in the weakly ordered regime: there exists a constant  $C$  such that  $1 - CLr^{L/2} \leq \vartheta^{(L)}(x, y) \leq 1$ .*

*Proof.* The first inequality  $\vartheta_L(x, y) \leq 1$  follows the same proof as in the differentiable case.

For the lower bound, using the fact that  $(1 - \beta)r = 1$ , we have  $\epsilon^{(\ell)} = 1 - \Sigma^{(\ell)}(x, y) \leq 2r^\ell$  and using the explicit value of  $R_{\dot{\sigma}}(\rho)$ , we get that  $R_{\dot{\sigma}}(\rho) \geq 1 - \sqrt{1 - \rho}$  which implies that  $\dot{\epsilon}^{(\ell)} = r - \dot{\Sigma}^{(\ell)}(x, y) \leq r\sqrt{2}r^{\frac{\ell-1}{2}}$ :

$$\begin{aligned} \Theta_\infty^{(L)}(x, y) &= \sum_{\ell=1}^L (1 - \epsilon^{(\ell)}) \prod_{k=\ell+1}^L r - \dot{\epsilon}^{(k)} \\ &\geq \sum_{\ell=1}^L r^{L-\ell} - 2r^{L-\ell}r^\ell - \sqrt{2} \sum_{k=\ell+1}^L r^{L-\ell-1+\frac{k-1}{2}} \\ &= \Theta_\infty^{(L)}(x, x) - 2Lr^L - \sqrt{2} \sum_{\ell=1}^L r^{L-\frac{\ell}{2}-1} \sum_{k=0}^{L-\ell-1} r^{\frac{k}{2}} \\ &\geq \Theta_\infty^{(L)}(x, x) - 2Lr^L - \frac{\sqrt{2}}{1 - \sqrt{r}} r^{L/2-1} \sum_{\ell=0}^{L-1} r^{\ell/2} \\ &= \Theta_\infty^{(L)}(x, x) - 2Lr^L - \frac{\sqrt{2}}{1 - \sqrt{r}} r^{L/2-1} \frac{1}{1 - \sqrt{r}} \\ &\geq \Theta_\infty^{(L)}(x, x) - 2Lr^L - \frac{\sqrt{2}}{(1 - \sqrt{r})^2} r^{L/2-1} \\ &\geq \Theta_\infty^{(L)}(x, x) - \left[ 2Lr^{L/2} - \frac{\sqrt{2}}{r(1 - \sqrt{r})^2} \right] r^{L/2} \\ &\geq \Theta_\infty^{(L)}(x, x) - C_0(r, \beta)r^{L/2}. \end{aligned}$$

Recall that for any  $x \in \mathbb{S}_{n_0}$ ,  $\Theta_\infty^{(L)}(x, x) = \frac{1-r^L}{1-r}$  is bounded in  $L$ . Dividing the previous inequality by  $\Theta_\infty^{(L)}(x, x)$  we get:  $1 - Cr^{L/2} \leq \vartheta_L(x, y) \leq 1$ .  $\square$

## C Layer Normalization and Nonlinearity Normalization

### C.1 Layer normalization asymptotically equivalent to nonlinearity normalization.

With Layer Normalization (LN), the coordinates of the normalized vectors of activations are  $\check{\alpha}_j^{(\ell)}(x) =$

$$\sqrt{n_\ell} \frac{\alpha_j^{(\ell)}(x) - \mu^{(\ell)}(x)}{\|\alpha^{(\ell)}(x) - \underline{\mu}^{(\ell)}(x)\|}, \text{ where } \mu^{(\ell)} := \frac{1}{n_\ell} \sum_{i=1}^{n_\ell} \alpha_i^{(\ell)}(x) \text{ and } \underline{\mu}^{(\ell)} := \begin{pmatrix} \mu^{(\ell)} \\ \vdots \\ \mu^{(\ell)} \end{pmatrix}. \text{ We simplify the}$$

notation by keeping the dependence on  $x$  implicate and denote the standardized nonlinearity  $\underline{\sigma}(\cdot) := \frac{\sigma(\cdot) - \mathbb{E}(\sigma(Z))}{\sqrt{\text{Var}(\sigma(Z))}}$ , where  $Z \stackrel{d}{\sim} \mathcal{N}(0, 1)$ .

Suppose that  $L = 2$ , that is we have a single hidden layer after which the LN is applied. More precisely, the output of the network function with LN is  $\tilde{\alpha}^{(2)}(\tilde{\alpha}^{(1)}(x))$ . We rewrite

$$\check{\alpha}^{(1)} = \sqrt{n_1} \frac{\sigma(\tilde{\alpha}^{(1)}) - \underline{\mu}^{(1)}}{\|\sigma(\tilde{\alpha}^{(1)}) - \underline{\mu}^{(1)}\|} = \underline{\sigma}(\tilde{\alpha}^{(1)})C_1 + C_2,$$

$$\text{where } C_1 = \sqrt{n_1} \frac{\sqrt{\text{Var}(\sigma(Z))}}{\|\sigma(\tilde{\alpha}^{(1)}) - \underline{\mu}^{(1)}\|}, \text{ and } C_2 = \sqrt{n_1} \frac{\mathbb{E}(\sigma(Z)) - \underline{\mu}^{(1)}}{\|\sigma(\tilde{\alpha}^{(1)}) - \underline{\mu}^{(1)}\|}.$$

Note that  $C_1 \rightarrow 1$  and  $C_2 \rightarrow 0$  almost surely, as  $n_1 \rightarrow \infty$ . Indeed, since the  $\tilde{\alpha}_i^{(1)}$ 's are independent standard Gaussian variables at initialization (recall that we assume that the inputs belong to  $\mathbb{S}_{n_0}$ ), the law of large numbers entails that  $\mu^{(1)} \rightarrow \mathbb{E}(\sigma(Z))$  almost surely, as  $n_1 \rightarrow \infty$ , and similarly for  $\frac{\|\sigma(\tilde{\alpha}^{(1)}) - \underline{\mu}^{(1)}\|^2}{n_1} \rightarrow \text{Var}(\sigma(Z))$ .

To show that LN is asymptotically equivalent to centering and standardizing the nonlinearity, we now establish that  $C_1$  and  $C_2$  are constant during training. We have

$$\frac{\partial}{\partial \tilde{\alpha}_j^{(1)}} \|\sigma(\tilde{\alpha}^{(1)}) - \underline{\mu}^{(1)}\| = \frac{\dot{\sigma}(\tilde{\alpha}_j^{(1)}) \sum_{i=1}^{n_1} (\delta_{ij} - 1/n_1) (\sigma(\tilde{\alpha}_i^{(1)}) - \underline{\mu}^{(1)})}{\|\sigma(\tilde{\alpha}^{(1)}) - \underline{\mu}^{(1)}\|} = \frac{\dot{\sigma}(\tilde{\alpha}_j^{(1)}) (\sigma(\tilde{\alpha}_j^{(1)}) - \underline{\mu}^{(1)})}{\|\sigma(\tilde{\alpha}^{(1)}) - \underline{\mu}^{(1)}\|}. \quad (\text{C.1})$$

Note that the absolute value of the latter is bounded by  $2\|\dot{\sigma}\|_\infty$ . We write  $g(t)$  for any function  $g$  that depends on the parameters  $\theta(t)$  at time  $t \geq 0$ . Using twice the triangle inequality yields that

$$\begin{aligned} \left| \|\sigma(\tilde{\alpha}^{(1)}(t)) - \underline{\mu}^{(1)}(t)\| - \|\sigma(\tilde{\alpha}^{(1)}(0)) - \underline{\mu}^{(1)}(0)\| \right| &\leq \|\sigma(\tilde{\alpha}^{(1)}(t)) - \sigma(\tilde{\alpha}^{(1)}(0))\| + \|\underline{\mu}^{(1)}(t) - \underline{\mu}^{(1)}(0)\| \\ &\leq \|\dot{\sigma}\|_\infty \left( \left( \sum_{i=1}^{n_1} (\tilde{\alpha}_i^{(1)}(t) - \tilde{\alpha}_i^{(1)}(0))^2 \right)^{1/2} + \frac{1}{\sqrt{n_1}} \sum_{i=1}^{n_1} |\tilde{\alpha}_i^{(1)}(t) - \tilde{\alpha}_i^{(1)}(0)| \right) \leq ct, \end{aligned} \quad (\text{C.2})$$

for some constant  $c > 0$ , where we used that  $|\tilde{\alpha}_i^{(1)}(t) - \tilde{\alpha}_i^{(1)}(0)| = \mathcal{O}(t/\sqrt{n_1})$ , see Appendix A.2 of [11]. Since  $\|\sigma(\tilde{\alpha}^{(1)}(0)) - \underline{\mu}^{(1)}(0)\| \sim \sqrt{n_1}$  by the law of large numbers, we can always write  $\|\sigma(\tilde{\alpha}^{(1)}(t)) - \underline{\mu}^{(1)}(t)\| > \|\sigma(\tilde{\alpha}^{(1)}(0)) - \underline{\mu}^{(1)}(0)\| - ct > 0$ . Hence, using (C.1) then (C.2), we get

$$\begin{aligned} \left| \frac{\partial C_1(t)}{\partial \tilde{\alpha}_j^{(1)}(t)} \right| &= \frac{\sqrt{n_1} \text{Var}(\sigma(Z))}{\|\sigma(\tilde{\alpha}^{(1)}(t)) - \underline{\mu}^{(1)}(t)\|^2} \cdot \left| \frac{\dot{\sigma}(\tilde{\alpha}_j^{(1)}(t)) (\sigma(\tilde{\alpha}_j^{(1)}(t)) - \underline{\mu}^{(1)}(t))}{\|\sigma(\tilde{\alpha}^{(1)}(t)) - \underline{\mu}^{(1)}(t)\|} \right| \\ &\leq \frac{\sqrt{n_1} \text{Var}(\sigma(Z))}{(\|\sigma(\tilde{\alpha}^{(1)}(0)) - \underline{\mu}^{(1)}(0)\| - ct)^2} \|\dot{\sigma}\|_\infty = \mathcal{O}(1/\sqrt{n_1}), \end{aligned} \quad (\text{C.3})$$

by the law of large numbers. The case of  $C_2$  is similar:

$$\begin{aligned} \frac{\partial C_2(t)}{\partial \tilde{\alpha}_j^{(1)}(t)} &= \frac{-\dot{\sigma}(\tilde{\alpha}_j^{(1)}(t))}{\sqrt{n_1} \|\sigma(\tilde{\alpha}^{(1)}(t)) - \underline{\mu}^{(1)}(t)\|} - \sqrt{n_1} \frac{(\mathbb{E}(\sigma(Z)) - \underline{\mu}^{(1)}(t)) \dot{\sigma}(\tilde{\alpha}_j^{(1)}(t)) (\sigma(\tilde{\alpha}_j^{(1)}(t)) - \underline{\mu}^{(1)}(t))}{\|\sigma(\tilde{\alpha}^{(1)}(t)) - \underline{\mu}^{(1)}(t)\|^3} \\ &\leq \|\dot{\sigma}\|_\infty \left( \frac{1}{n_1} \frac{\sqrt{n_1}}{\|\sigma(\tilde{\alpha}^{(1)}(0)) - \underline{\mu}^{(1)}(0)\| - ct} - \frac{1}{\sqrt{n_1}} \frac{n_1 (\mathbb{E}(\sigma(Z)) - \underline{\mu}^{(1)}(0) + ct)}{(\|\sigma(\tilde{\alpha}^{(1)}(0)) - \underline{\mu}^{(1)}(0)\| - ct)^2} \right) = \mathcal{O}(1/\sqrt{n_1}), \end{aligned} \quad (\text{C.4})$$



again by the law of large numbers. For  $i = 1, 2$ , we now write  $\frac{\partial C_i(t)}{\partial t} = \frac{\partial \tilde{\alpha}_j^{(1)}(t)}{\partial t} \frac{\partial C_i(t)}{\partial \tilde{\alpha}_j^{(1)}(t)}$  and recall that the first term is changing at rate  $\mathcal{O}(1/\sqrt{n_1})$ . Therefore,  $|C_i(t) - C_i(0)| \leq \mathcal{O}(t/n_1)$ . The claim for  $L \geq 3$  follows by induction.

## C.2 Pre-layer normalization has asymptotically no effect.

Normalizing the preactivations has asymptotically no effect on the network at initialization as well as during training. The output of the  $\ell$ -th layer becomes  $\tilde{\alpha}_j^{(\ell)} = \sigma(\sqrt{n_\ell} \frac{\tilde{\alpha}_j^{(\ell)} - \mu^{(\ell)}}{\|\tilde{\alpha}^{(\ell)} - \underline{\mu}^{(\ell)}\|})$  where  $\mu^{(\ell)}$  and  $\underline{\mu}^{(\ell)}$  are computed similarly as before with  $\tilde{\alpha}^{(\ell)}$  in place of  $\alpha^{(\ell)}$ . As before, we assume  $L = 2$  and deduce the general case by induction. We write  $\tilde{\alpha}_j^{(1)} = \sigma(\tilde{\alpha}_j^{(1)} C_1 + C_2)$ , with  $C_1 = \sqrt{n_1}/\|\tilde{\alpha}^{(1)} - \underline{\mu}^{(1)}\|$  and  $C_2 = -\sqrt{n_1}\mu^{(1)}/\|\tilde{\alpha}^{(1)} - \underline{\mu}^{(1)}\|$ . Again, the law of large numbers show that  $C_1 \rightarrow 1$  and  $C_2 \rightarrow 0$  almost surely, as  $n_1 \rightarrow \infty$ . Moreover, similarly as (C.1) and (C.2), we have that

$$\begin{aligned} \frac{\partial}{\partial \tilde{\alpha}_j^{(1)}} \|\tilde{\alpha}^{(1)} - \underline{\mu}^{(1)}\| &= \frac{\tilde{\alpha}_j^{(1)} - \mu^{(1)}}{\|\tilde{\alpha}^{(1)} - \underline{\mu}^{(1)}\|}, \\ \left| \|\tilde{\alpha}^{(1)}(t) - \underline{\mu}^{(1)}(t)\| - \|\tilde{\alpha}^{(1)}(0) - \underline{\mu}^{(1)}(0)\| \right| &\leq ct, \end{aligned}$$

for some constant  $c > 0$ . Using the same argument as in (C.3) and (C.4), one can thus show for  $i = 1, 2$  that

$$\left| \frac{\partial C_i(t)}{\partial \tilde{\alpha}_j^{(1)}} \right| = \mathcal{O}(1/\sqrt{n_1}).$$

We conclude as previously, noting that

$$\frac{\partial \tilde{\alpha}_j^{(1)}(t)}{\partial t} = \dot{\sigma} \left( \tilde{\alpha}_j^{(1)}(t) C_1(t) + C_2(t) \right) \left( \frac{\partial \tilde{\alpha}_j^{(1)}(t)}{\partial t} C_1(t) + \tilde{\alpha}_j^{(1)}(t) \frac{\partial C_1(t)}{\partial t} + \frac{\partial C_2(t)}{\partial t} \right).$$

## D Batch Normalization

If one adds a BatchNorm layer after the nonlinearity of the last hidden layer, we have:

**Lemma 14.** *Consider a FC-NN with  $L$  layers, with a PN-BN after the last nonlinearity. For any  $k, k' \in \{1, \dots, n_L\}$  and any parameter  $\theta_p$ , we have  $\sum_{i=1}^N \Theta_{\theta_p}^{(L)}(\cdot, x_i) = \beta^2 \text{Id}_{n_L}$ .*

*Proof.* This is an direct consequence of the definition of the NTK and of the following claim:

*Claim.* For a fully-connected DNN with a BatchNorm layer after the nonlinearity of the last hidden layer then  $\frac{1}{N} \sum_{i=1}^N \partial_{\theta_p} f_{\theta, k}(x_i)$  is equal to  $\beta$  if  $\theta_p$  is  $b_k^{(L-1)}$ , the bias parameter of the last layer, and equal to 0 otherwise.

The average of  $f_{\theta, k}$  on the training set,  $\frac{1}{N} \sum_{i=1}^N \partial_{\theta_p} f_{\theta, k}(x_i)$ , only depends on the bias of the last layer:

$$\frac{1}{N} \sum_{i=1}^N f_{\theta, k}(x_i) = \frac{\sqrt{1 - \beta^2}}{\sqrt{n_{L-1}}} W^{(L-1)} \frac{1}{N} \sum_{i=1}^N \hat{\alpha}^{(L-1)}(x_i) + \beta b_k^{(L-1)} = \beta b_k^{(L-1)}.$$

Thus for any parameter  $\theta_p$ ,  $\frac{1}{N} \sum_{i=1}^N \partial_{\theta_p} f_{\theta, k}(x_i) = \partial_{\theta_p} (\beta b_k^{(L-1)})$  is equal to  $\beta$  if the parameter is the bias  $b_k^{(L-1)}$  and zero otherwise.  $\square$

## E Graph-based Neural Networks

In this section, we prove the convergence of the NTK at initialization for a general family of DNNs which contain in particular CNNs and DC-NNs. We will consider the Graph-based parametrization introduced in the main.

For each layer  $\ell = 0, \dots, L$ , the neurons are indexed by a position  $p \in I_\ell$  and a channel  $i = 1, \dots, n_\ell$ . We may assume that the sets of positions  $I_\ell$  can be any set, in particular any subset of  $\mathbb{Z}^D$ . For any position  $p \in I_{\ell+1}$ , we consider a set of parents  $P(p) \subset I_\ell$  and we define recursively the set  $P^{\circ k}(p) \subset I_{\ell+1-k}$  of ancestors of level  $k$  by  $P^{\circ k}(p) = \{q \mid \exists q' \in P^{\circ k-1}(p), q \in P(q')\}$ . For each parent  $q \in P(p)$ , the connections from the position  $(q, \ell)$  to the position  $(p, \ell+1)$  are encoded in an  $n_\ell \times n_{\ell+1}$  weight matrix  $W^{(\ell, q \rightarrow p)}$ . We define  $\chi(q \rightarrow p, q' \rightarrow p')$  which is equal to 1 if and only if  $W^{(\ell, q \rightarrow p)}$  and  $W^{(\ell, q' \rightarrow p')}$  are shared (in the sense that the two matrices are forced to be equal at initialization and during training) and 0 otherwise. It satisfies  $\chi(q \rightarrow p, q \rightarrow p) = 1$  for any neuron  $p$  and any  $q \in P(p)$  and it is transitive. We will also suppose that for any neuron  $p$  and any  $q, q' \in P(p)$ ,  $\chi(q \rightarrow p, q' \rightarrow p) = \delta_{qq'}$  (i.e. no pair of connections connected to the same neuron  $p$  are shared).

In this setting, the activations and preactivations  $\alpha^{(\ell)}, \tilde{\alpha}^{(\ell)} \in (\mathbb{R}^{n_\ell})^{I_\ell}$  are recursively constructed using the parent-based NTK parametrization: we set  $\alpha^{(0)}(x) = x$  and for  $\ell = 0, \dots, L-1$  and any position  $p \in I_\ell$ :

$$\tilde{\alpha}^{(\ell+1, p)}(x) = \beta b^{(\ell)} + \frac{\sqrt{1-\beta^2}}{\sqrt{|P(p)|} n_\ell} \sum_{q \in P(p)} W^{(\ell, q \rightarrow p)} x_q, \quad \alpha^{(\ell+1)}(x) = \sigma\left(\tilde{\alpha}^{(\ell+1)}(x)\right)$$

where  $\sigma$  is applied entry-wise,  $\beta \geq 0$  and  $|P(p)|$  is the cardinal of  $P(p)$ . This is a slightly more general formalism than the DC-NNs and it will allow us to obtain simpler formulae which generalize well to other architectures.

*Remark 15.* Notice that the parametrization is slightly different than the traditional one: we divide by  $\sqrt{|P(p)|} n_\ell$  instead of dividing by  $\sqrt{n_\ell^{|\omega|/s_1 \dots s_d}}$ . This does not lead to any difference when one consider infinite-sized images as in Section F since in this case the number of parents is constant, equal to  $|\omega|/s_1 \dots s_d$ . The key difference between the two parametrizations will be investigated in Section G.

Recall, that for a kernel  $K : \mathbb{R}^{n_0} \times \mathbb{R}^{n_0} \rightarrow \mathbb{R}$ , and for any  $z_0, z_1 \in \mathbb{R}^{n_0}$ , we defined:

$$\mathbb{L}_K^g(z_0, z_1) = \mathbb{E}_{(y_0, y_1) \sim \mathcal{N}(0, (K(z_i, z_j))_{i,j=0,1})} [g(y_0) g(y_1)].$$

**Proposition 16.** *In this setting, as  $n_1 \rightarrow \infty, \dots, n_{\ell-1} \rightarrow \infty$  sequentially, the preactivations  $(\tilde{\alpha}_i^{(\ell, p)}(x))_{i=1, \dots, n_\ell, p \in I_\ell}$  of the  $\ell^{\text{th}}$  layer converge to a centered Gaussian process with covariance  $\Sigma^{(\ell, pp')}(x, y) \delta_{ii'}$ , where  $\Sigma^{(\ell, pp')}(x, y)$  is defined recursively as*

$$\begin{aligned} \Sigma^{(1, pp')}(x, y) &= \beta^2 + \frac{1-\beta^2}{\sqrt{|P(p)|} |P(p')| n_0} \sum_{q \in P(p)} \sum_{q' \in P(p')} \chi(q \rightarrow p, q' \rightarrow p') (x_q)^T y_{q'}, \\ \Sigma^{(\ell+1, pp')}(x, y) &= \beta^2 + \frac{1-\beta^2}{\sqrt{|P(p)|} |P(p')|} \sum_{q \in P(p)} \sum_{q' \in P(p')} \chi(q \rightarrow p, q' \rightarrow p') \mathbb{L}_{\Sigma^{(\ell, qq')}}^\sigma(x, y). \end{aligned}$$

*Proof.* The proof is done by induction on  $\ell$ . For  $\ell = 1$  and any  $i \in \{1, \dots, n_1\}$ , the preactivation

$$\tilde{\alpha}_i^{(1, p)}(x) = \beta b_i^{(0)} + \frac{\sqrt{1-\beta^2}}{\sqrt{|P(p)|} n_0} \sum_{q \in P(p)} \left( W_p^{(0, q \rightarrow p)} x_q \right)_i$$

is a random affine function of  $x$  and its coefficients are centered Gaussian: it is hence a centered Gaussian process whose covariance is easily shown to be equal to  $\mathbb{E} \left[ \tilde{\alpha}_i^{(1, p)}(x) \tilde{\alpha}_{i'}^{(1, p')}(y) \right] = \Sigma^{(1, pp')}(x, y) \delta_{ii'}$ .

For the induction step, we assume that the result holds for the pre-activations of the layer  $\ell$ . The pre-activations of the next layer are of the form

$$\tilde{\alpha}_i^{(\ell+1, p)}(x) = \beta b_i^{(0)} + \frac{\sqrt{1-\beta^2}}{\sqrt{|P(p)|} n_\ell} \sum_{q \in P(p)} \left( W^{(\ell, q \rightarrow p)} \alpha^{(\ell, q)}(x) \right)_i.$$

Conditioned on the activations  $\alpha^{(\ell,q)}$  of the last layer,  $\tilde{\alpha}^{(\ell+1,p)}$  is a centered Gaussian process: in other terms, it is a mixture of centered Gaussians with a random covariance determined by the activations of the last layer. The random covariance between  $\tilde{\alpha}_{i_0}^{(\ell+1,p_0)}(x)$  and  $\tilde{\alpha}_{i_1}^{(\ell+1,p_1)}(y)$  is equal to

$$\begin{aligned} & \beta^2 \delta_{i_0 i_1} + \frac{1 - \beta^2}{\sqrt{|P(p_0)||P(p_1)|}^{n_\ell}} \sum_{\substack{q_0 \in P(p_0) \\ q_1 \in P(p_1)}} \sum_{j_0, j_1=1}^{n_\ell} \mathbb{E} \left[ W_{i_0 j_0}^{(\ell, q_0 \rightarrow p_0)} W_{i_1 j_1}^{(\ell, q_1 \rightarrow p_1)} \right] \alpha_{j_0}^{(\ell, q_0)}(x) \alpha_{j_1}^{(\ell, q_1)}(y) \\ &= \delta_{i_0 i_1} \left[ \beta^2 + \frac{1 - \beta^2}{\sqrt{|P(p_0)||P(p_1)|}^{n_\ell}} \sum_{\substack{q_0 \in P(p_0) \\ q_1 \in P(p_1)}} \chi(q_0 \rightarrow p_0, q_1 \rightarrow p_1) \frac{1}{n_\ell} \sum_{j=1}^{n_\ell} \sigma \left( \tilde{\alpha}_j^{(\ell, q_0)}(x) \right) \sigma \left( \tilde{\alpha}_j^{(\ell, q_1)}(y) \right) \right], \end{aligned}$$

where we used the fact that  $\mathbb{E} \left[ W_{i_0 j_0}^{(\ell, q_0 \rightarrow p_0)} W_{i_1 j_1}^{(\ell, q_1 \rightarrow p_1)} \right] = \chi(q_0 \rightarrow p_0, q_1 \rightarrow p_1) \delta_{i_0 i_1} \delta_{j_0 j_1}$ . Using the induction hypothesis, as  $n_1 \rightarrow \infty, \dots, n_{\ell-1} \rightarrow \infty$  sequentially, the preactivations  $\left( \tilde{\alpha}_j^{(\ell, q_0)}(x), \tilde{\alpha}_j^{(\ell, q_1)}(y) \right)_j$  converge to independant centered Gaussian pairs. As  $n_\ell \rightarrow \infty$ , by the law of large numbers, the sum over  $j$  along with the  $1/n_\ell$  converges to  $\mathbb{L}_{\sigma}^{\Sigma^{(\ell, qq')}}(x, y)$ . In this limit, the random covariance of the Gaussian mixture becomes deterministic and as a consequence, the mixture of Gaussian processes tends to a centered Gaussian process with the right covariance.  $\square$

Similarly to the activation kernels, one can prove that the NTK converges at initialization.

**Proposition 17.** *As  $n_1 \rightarrow \infty, \dots, n_{L-1} \rightarrow \infty$  sequentially, the NTK  $\Theta^{(L, p_0 p_1)}$  of a general convolutional network converges to  $\Theta_{\infty, p_0 p_1}^{(L)} \otimes \text{Id}_{n_L}$  where  $\Theta_{\infty}^{(L, p_0 p_1)}(x, y)$  is defined recursively by:*

$$\begin{aligned} \Theta_{\infty}^{(1, p_0 p_1)}(x, y) &= \Sigma^{(1, p_0 p_1)}(x, y), \\ \Theta_{\infty}^{(L, p_0 p_1)}(x, y) &= \frac{1 - \beta^2}{\sqrt{|P(p_0)||P(p_1)|}^{n_L}} \sum_{\substack{q_0 \in P(p_0) \\ q_1 \in P(p_1)}} \chi(q_0 \rightarrow p_0, q_1 \rightarrow p_1) \Theta_{\infty}^{(L-1, q_0 q_1)}(x, y) \mathbb{L}_{\Sigma^{(L-1, q_0 q_1)}}^{\dot{\sigma}}(x, y) \\ &+ \Sigma^{(L, p_0 p_1)}(x, y). \end{aligned}$$

*Proof.* The proof by induction on  $L$  follows the one of [11] for fully-connected DNNs. We present the induction step and assume that the result holds for a general convolutional network with  $L - 1$  hidden layers. Following the same computations as in [11], the NTK  $\Theta_{p_0 p_1, j j'}^{(L+1)}(x, y)$  is equal to

$$\begin{aligned} & \frac{1 - \beta^2}{\sqrt{|P(p_0)||P(p_1)|}^{n_L}} \sum_{q_0 \in P(p_0)} \sum_{q_1 \in P(p_1)} \sum_{ii'} \Theta_{ii'}^{(L, q_0 q_1)}(x, y) \dot{\sigma} \left( \tilde{\alpha}_i^{(L, q_0)}(x) \right) \dot{\sigma} \left( \tilde{\alpha}_{i'}^{(L, q_1)}(y) \right) \\ & \quad W_{ij}^{(L, q_0 \rightarrow p_0)} W_{i'j'}^{(L, q_1 \rightarrow p_1)} \\ & + \delta_{jj'} \beta^2 + \delta_{jj'} \frac{1 - \beta^2}{\sqrt{|P(p_0)||P(p_1)|}^{n_L}} \sum_{q_0 \in P(p_0)} \sum_{q_1 \in P(p_1)} \chi(q_0 \rightarrow p_0, q_1 \rightarrow p_1) \sum_i \alpha_i^{(L, q_0)}(x) \alpha_i^{(L, q_1)}(y) \end{aligned}$$

which, by assumption, converges as  $n_1 \rightarrow \infty, \dots, n_{L-1} \rightarrow \infty$  to

$$\begin{aligned} & \frac{1 - \beta^2}{\sqrt{|P(p_0)||P(p_1)|}^{n_L}} \sum_{q_0 \in P(p_0)} \sum_{q_1 \in P(p_1)} \sum_i \Theta_{\infty}^{(L, q_0 q_1)}(x, y) \dot{\sigma} \left( \tilde{\alpha}_i^{(L, q_0)}(x) \right) \dot{\sigma} \left( \tilde{\alpha}_i^{(L, q_1)}(y) \right) \\ & \quad W_{ij}^{(L, q_0 \rightarrow p_0)} W_{i'j'}^{(L, q_1 \rightarrow p_1)} \\ & + \delta_{jj'} \beta^2 + \delta_{jj'} \frac{1 - \beta^2}{\sqrt{|P(p_0)||P(p_1)|}^{n_L}} \sum_{q_0 \in P(p_0)} \sum_{q_1 \in P(p_1)} \chi(q_0 \rightarrow p_0, q_1 \rightarrow p_1) \sum_i \alpha_i^{(L, q_0)}(x) \alpha_i^{(L, q_1)}(y). \end{aligned}$$

As  $n_L \rightarrow \infty$ , using the previous results on the preactivations and the law of large number, the NTK converges to

$$\begin{aligned} & \frac{1 - \beta^2}{\sqrt{|P(p_0)||P(p_1)|}} \sum_{q_0 \in P(p_0)} \sum_{q_1 \in P(p_1)} \Theta_\infty^{(L, q_0 q_1)}(x, y) \mathbb{L}_{\Sigma^{(L, q_0 q_1)}}^{\dot{\sigma}}(x, y) \mathbb{E} \left[ W_{ij}^{(L, q_0 \rightarrow p_0)} W_{ij'}^{(L, q_1 \rightarrow p_1)} \right] \\ & + \delta_{jj'} \beta^2 + \delta_{jj'} \frac{1 - \beta^2}{\sqrt{|P(p_0)||P(p_1)|}} \sum_{q_0 \in P(p_0)} \sum_{q_1 \in P(p_1)} \chi(q_0 \rightarrow p_0, q_1 \rightarrow p_1) \mathbb{L}_{\Sigma^{(L, q_0 q_1)}}^{\sigma}(x, y), \end{aligned}$$

which can be simplified—using the fact that  $\mathbb{E} \left[ W_{ij}^{(L, q_0 \rightarrow p_0)} W_{ij'}^{(L, q_1 \rightarrow p_1)} \right] = \chi(q_0 \rightarrow p_0, q_1 \rightarrow p_1) \delta_{jj'}$ —into:

$$\begin{aligned} & \delta_{jj'} \frac{1 - \beta^2}{\sqrt{|P(p_0)||P(p_1)|}} \sum_{q_0 \in P(p_0)} \sum_{q_1 \in P(p_1)} \chi(q_0 \rightarrow p_0, q_1 \rightarrow p_1) \Theta_\infty^{(L, q_0 q_1)}(x, y) \mathbb{L}_{\Sigma^{(L, q_0 q_1)}}^{\dot{\sigma}}(x, y) \\ & + \delta_{jj'} \Sigma^{(L+1, p_0 p_1)}(x, y), \end{aligned}$$

which proves the assertions.  $\square$

## F DC-NN Order and Chaos

In this section, in order to study the behaviour of DC-NNs in the bulk and to avoid dealing with border effects, studied in Section G, we assume that for all layers  $\ell$  there is no border, i.e. the positions  $p$  are in  $\mathbb{Z}^d$ . Let us consider a DC-NN with up-sampling  $s \in \{2, 3, \dots\}^d$  where the window sizes for all layers are all set equal to  $\pi = \omega = \{0, \dots, w_1 s_1 - 1\} \times \dots \times \{0, \dots, w_d s_d - 1\}$ . A position  $p$  has therefore  $w_1 \cdots w_d$  parents which are given by

$$P(p) = \{ \lfloor p_0/s_0 \rfloor, \lfloor p_0/s_0 \rfloor + 1, \dots, \lfloor p_0/s_0 \rfloor + w_1 \} \times \dots \times \{ \lfloor p_d/s_d \rfloor, \lfloor p_d/s_d \rfloor + 1, \dots, \lfloor p_d/s_d \rfloor + w_d \}.$$

Two connections  $q \rightarrow p$  and  $q' \rightarrow p'$  are shared if and only if  $s \mid p - p'$  (i.e. for any  $i = 1, \dots, d$ ,  $s_i \mid p_i - p'_i$ ) and  $q_i - q'_i = \frac{p_i - p'_i}{s_i}$  for any  $i = 1, \dots, d$ .

Propositions 16 and 17 hold true in this setting. By Proposition 22, if the nonlinearity  $\sigma$  is standardized,  $\Sigma^{(\ell, pp)}(x, x) = 1$  for any  $x \in \mathbb{S}_{n_0}^{I_0}$  and any  $p \in I_\ell$ . The activation kernels  $\Sigma^{(\ell, pp')}(x, y)$  for any two inputs  $x, y \in \mathbb{S}_{n_0}^{I_0}$  and two output positions  $p, p' \in \mathbb{Z}^d$  are therefore defined recursively by:

$$\begin{aligned} \Sigma^{(1, pp')}(x, y) &= \beta^2 + \delta_{s \mid p - p'} \frac{1 - \beta^2}{|P(p)| n_0} \sum_{q \in P(p)} (x_q)^T y_{q + \frac{p' - p}{s}}, \\ \Sigma^{(\ell+1, pp')}(x, y) &= \beta^2 + \delta_{s \mid p - p'} \frac{1 - \beta^2}{|P(p)|} \sum_{q \in P(p)} R_\sigma \left( \Sigma^{(\ell, q, q + \frac{p' - p}{s})}(x, y) \right), \end{aligned}$$

where  $\frac{p' - p}{s} = \left( \frac{p'_i - p_i}{s_i} \right)_i$  is a valid position since  $s \mid p - p'$ . Similarly, the NTK at initialization satisfies the following recursion:

$$\Theta_\infty^{(L+1, pp')}(x, y) = \Sigma^{(L+1, pp')}(x, y) + \delta_{s \mid p - p'} \frac{1 - \beta^2}{|P(p)|} \sum_{q \in P(p)} \Theta_\infty^{(L, q, q + \frac{p' - p}{s})}(x, y) R_\sigma \left( \Sigma^{(L, q, q + \frac{p' - p}{s})}(x, y) \right).$$

*Remark.* Recall that the  $s$ -valuation  $v_s(n)$  of a number  $n \in \mathbb{Z}^d$  is the largest  $k \in \{0, 1, 2, \dots\}$  such that  $s_i^k \mid n_i$  for all dimensions  $i = 1, \dots, d$ . For two pixels  $p, p' \in \mathbb{Z}^d$  and any input vectors  $x, y \in \mathbb{S}_{n_0}^{I_0}$ , if  $v_s(p' - p) < \ell$  the activation kernel  $\Sigma^{(\ell, pp')}(x, y)$  does not depend neither on  $x$  nor on  $y$ . More precisely, if  $v = v_s(p' - p) = 0$ , we have

$$\Sigma^{(\ell, pp')}(x, y) = \beta^2,$$

and for a general  $v < \ell$ :

$$c_v := \Sigma^{(\ell, pp')}(x, y) = (B_\beta \circ R_\sigma)^{\circ v}(\beta^2).$$

In particular, if  $v < L$ , the NTK is therefore also equal to a constant:

$$\Theta_\infty^{(L, pp')}(x, y) = \sum_{k=0}^v c_k (1 - \beta^2)^k \prod_{m=0}^{k-1} R_{\dot{\sigma}}(c_m).$$

We establish the bounds on the rate of convergence in the ‘‘order’’ region and on the values of the activations kernel in the chaos region for DC-NNs.

**Proposition 18.** *In the setting introduced above, for a standardized twice differentiable  $\sigma$ , for  $x, y \in \mathbb{S}_{n_0}^{I_0}$ , and any positions  $p, p' \in I_\ell$ , taking  $k = \min\{v_s(p' - p), \ell\}$ , we have:*

If  $r_{\sigma, \beta} < 1$  then:

$$1 \geq \Sigma^{(\ell, pp')}(x, y) \geq 1 - 2(1 - \beta^2)r_{\sigma, \beta}^k.$$

If  $r_{\sigma, \beta} > 1$  then there exists a fixed point  $a \in [0, 1)$  of  $B_\beta \circ R_\sigma$  such that:

- If  $k < \ell$ :

$$\left| \Sigma^{(\ell, pp')}(x, y) \right| \leq \max\{\beta^2, a\},$$

- If  $p' - p = ms^\ell$  and there is a  $c \leq 1$  such that for all input positions  $q \in P^{\circ \ell}(p)$ ,  $\left| \frac{1}{n_0} x_q^T y_{q+m} \right| \leq c$ , then

$$\left| \Sigma^{(\ell, pp')}(x, y) \right| \leq \max\{\beta^2 + (1 - \beta^2)c, a\}.$$

*Proof.* Let us denote  $r = r_{\sigma, \beta}$ . Let us suppose that  $r < 1$  and let us prove the first assertion by induction on  $\ell$ . If  $\ell = 1$ , then

$$\begin{aligned} \Sigma^{(1, pp')}(x, y) &= \beta^2 + \delta_{s|p-p'} \frac{1 - \beta^2}{|P(p)| n_0} \sum_{q \in P(p)} (x_q)^T y_{q + \frac{p'-p}{s}} \\ &\geq \beta^2 - \delta_{s|p-p'} (1 - \beta^2) \\ &\geq 1 - 2(1 - \beta^2) \end{aligned}$$

For the induction step, if we suppose that the inequality holds true for  $\ell$ , then

$$\begin{aligned} \Sigma^{(\ell+1, pp')}(x, y) &\geq \beta^2 + \delta_{s|p-p'} \frac{1 - \beta^2}{|P(p)|} \sum_{q=0}^{w/s} R_\sigma(1 - 2(1 - \beta^2)r^{k-1}) \\ &\geq \beta^2 + \delta_{s|p-p'} \frac{1 - \beta^2}{|P(p)|} \sum_{q=0}^{w/s} 1 - 2(1 - \beta^2)R_{\dot{\sigma}}(1)r^{k-1} \\ &\geq \beta^2 + \delta_{s|p-p'} (1 - \beta^2 - 2(1 - \beta^2)r^k) \\ &= \begin{cases} 1 - (1 - \beta^2) & \text{if } k = 0 \\ 1 - 2(1 - \beta^2)r^k & \text{if } k > 0 \end{cases} \\ &\geq 1 - 2(1 - \beta^2)r^k \end{aligned}$$

Now let us suppose that  $r > 1$ . If  $k < \ell$ , then  $\left| \Sigma^{(\ell, pp')}(x, y) \right| = \left| (B_\beta \circ R_\sigma)^{\circ k}(\beta^2) \right| < \max\{\beta^2, a\}$ . Let us suppose at last that  $k = \ell$  and let us prove the last assertion by induction on  $\ell$ . If  $\ell = 1$ , then

$$\begin{aligned} \left| \Sigma^{(1, pp')}(x, y) \right| &\leq \beta^2 + \frac{1 - \beta^2}{|P(p)| n_0} \sum_{q \in P(p)} \left| x_q^T y_{q + \frac{p'-p}{s}} \right| \\ &\leq \beta^2 + \frac{1 - \beta^2}{|P(p)|} \sum_{q \in P(p)} c \\ &= \beta^2 + (1 - \beta^2)c. \end{aligned}$$

For the induction step, if we suppose that the inequality holds true for  $\ell$ , then

$$\begin{aligned}
\left| \Sigma^{(\ell+1, pp')}(x, y) \right| &\leq \beta^2 + \frac{(1-\beta^2)}{|P(p)|} \sum_{q \in P(p)} \left| R_\sigma \left( \Sigma^{(\ell, q, q + \frac{p'-p}{s})(x, y)} \right) \right| \\
&\leq \beta^2 + \frac{(1-\beta^2)}{|P(p)|} \sum_{q \in P(p)} R_\sigma \left( \max\{\beta^2 + (1-\beta^2)c, a\} \right) \\
&= B_\beta \circ R_\sigma \left( \max\{\beta^2 + (1-\beta^2)c, a\} \right) \\
&\leq \max\{\beta^2 + (1-\beta^2)c, a\},
\end{aligned}$$

which allow us to conclude.  $\square$

The NTK features the same two regimes:

**Theorem 19.** Take  $I_0 = \mathbb{Z}^d$ , and consider a DC-NN with upsampling stride  $s \in \{2, 3, \dots\}^d$ , windows  $\pi_\ell = \omega_\ell = \{0, \dots, w_1 s_1 - 1\} \times \dots \times \{0, \dots, w_d s_d - 1\}$  for  $w \in \{1, 2, 3, \dots\}^d$ . For a standardized twice differentiable  $\sigma$ , there exist constants  $C_1, C_2 > 0$ , such that the following holds: for  $x, y \in \mathbb{S}_{n_0}^{I_0}$ , and any positions  $p, p' \in I_L$ , we have:

**Order:** When  $r_{\sigma, \beta} < 1$ , taking  $v = \min(v_s(p-p'), L-1)$ , taking  $v = L-1$  if  $p = p'$  and  $r = r_{\sigma, \beta}$ , we have

$$\frac{1-r^{v+1}}{1-r^L} - C_1(v+1)r^v \leq \vartheta_\infty^{(L, p, p')}(x, y) \leq \frac{1-r^{v+1}}{1-r^L}.$$

**Chaos:** When  $r_{\sigma, \beta} > 1$ , if either  $v_s(p-p') < L$  or if there exists a  $c < 1$  such that for all positions  $q \in I_0$  which are ancestor of  $p$ ,  $\left| x_q^T y_{q + \frac{p'-p}{s}} \right| < c$ , then there exists  $h < 1$  such that

$$\left| \vartheta_\infty^{(L, p, p')}(x, y) \right| \leq C_2 h^L.$$

*Proof.* Let us denote  $r = r_{\sigma, \beta}$  and let us suppose that  $r < 1$ . The NTK can be bounded recursively

$$\begin{aligned}
\Theta_\infty^{(L, pp')}(x, y) &= \Sigma^{(L, pp')}(x, y) + \delta_{s|p-p'} \frac{1-\beta^2}{|P(p)|} \sum_{q \in P(p)} \Theta_\infty^{(L-1, q, q + \frac{p'-p}{s})(x, y)} R_\sigma \left( \Sigma^{(L-1, q, q + \frac{p'-p}{s})(x, y)} \right) \\
&\geq 1 - 2(1-\beta^2)r^v + \delta_{s|p-p'} \frac{1}{|P(p)|} \sum_{q \in P(p)} \Theta_\infty^{(L, q, q + \frac{p'-p}{s})(x, y)} (r - \psi 2(1-\beta^2)^2 r^{v-1}).
\end{aligned}$$

Unrolling this inequality, we get:

$$\begin{aligned}
\Theta_\infty^{(L, pp')}(x, y) &= \sum_{k=0}^v (1 - 2(1-\beta^2)r^k) \prod_{m=k+1}^v (r - \psi 2(1-\beta^2)^2 r^{m-1}) \\
&\geq \sum_{k=0}^v r^{v-k} - 2(1-\beta^2)r^{v-k} r^k - \psi 2(1-\beta^2)^2 \sum_{m=k+1}^v r^{v-k-1} r^{m-1} \\
&= \frac{1-r^{v+1}}{1-r} - 2(1-\beta^2)(v+1)r^v - \psi 2(1-\beta^2)^2 \sum_{k=0}^v r^{v-1} \sum_{m=0}^{v-k-1} r^m \\
&\geq \frac{1-r^{v+1}}{1-r} - 2(1-\beta^2) \left[ r + \frac{\psi(1-\beta^2)}{1-r} \right] (v+1)r^{v-1} \\
&\geq \frac{1-r^{v+1}}{1-r} - C_{\sigma, \beta}(v+1)r^v.
\end{aligned}$$

For the upper bound, we have:  $\Theta_\infty^{(L, pp')}(x, y) \leq \sum_{\ell=L-k}^L 1 \prod_{m=\ell+1}^L r = \frac{1-r^{v+1}}{1-r}$ . Thus, we get the same bounds as in the FC-NNs case, but with respect to  $v$ , which is the maximal integer strictly smaller than  $L$  such that  $s^v |p-p'|$ :

$$\frac{1-r^{v+1}}{1-r} \geq \Theta_\infty^{(L, pp')}(x, y) \geq \frac{1-r^{v+1}}{1-r} - C(v+1)r^v.$$

Dividing by  $\Theta_\infty^{(L,pp)}(x, x)$  which is bounded in the ordered regime (see proof of Proposition 22) as  $L \rightarrow \infty$ , one gets the desired result.

If  $r > 1$ , there are two cases. When  $p' - p = ks^L$  then if there exists  $c < 1$  such that  $|x_q^T y_{q+k}| < cn_0$  for all ancestors  $q$  of  $p$ . Writing  $z = \max\{\beta^2 + (1 - \beta^2)c, a\}$  and  $w = (1 - \beta^2)R_\sigma(z) < r$  such that  $|\Sigma^{(\ell; q, q+ks^\ell)}(x, y)| < z$  for all position  $q$  at layer  $\ell$  which is an ancestor of  $p$ . Then

$$\left| \Theta_\infty^{(L,pp')} (x, y) \right| \leq \sum_{\ell=1}^L vw^{L-\ell} = v \frac{1-w^L}{1-w}$$

such that

$$\frac{\left| \Theta_\infty^{(L,pp')} (x, y) \right|}{\left| \Theta_\infty^{(L,pp)} (x, x) \right|} \leq c \frac{1-r}{1-w} \frac{1-w^L}{1-r^L} \leq C(\sigma, \beta) \left( \frac{w}{r} \right)^L$$

which goes to zero exponentially.

If  $p' - p$  is not divisible by  $s^L$  then for  $z = \max\{\beta^2, a\}$  and  $w = (1 - \beta^2)R_\sigma(z) < r$

$$\left| \Theta_\infty^{(L,pp')} (x, y) \right| \leq \sum_{\ell=L-v+1}^L zw^{L-\ell} = z \frac{1-w^v}{1-w}$$

which also converges exponentially to 0. □

## F.1 Adapting the learning rate

Let us suppose that we multiply the learning rate of the  $\ell$ -th layer weights and bias by  $S^{-\frac{\ell}{2}}$  where  $S = \prod_i s_i$ . This is slightly different than what we propose in the main, where the learning rate of the bias are multiplied by  $S^{-\frac{\ell+1}{2}}$  instead of  $S^{-\frac{\ell}{2}}$ , but it greatly simplifies the formulas. Furthermore, the balance between the weights and bias can be modified with the meta-parameter  $\beta$  to achieve a similar result. The NTK then takes the value:

$$\begin{aligned} \Theta^{(L,pp)}(x, x) &= \sum_{\ell=1}^L S^{-\frac{\ell}{2}} \prod_{n=\ell+1}^L r \\ &= \sum_{\ell=1}^L S^{-\frac{\ell}{2}} r^{L-\ell} \\ &= \sum_{\ell=0}^{L-1} S^{-\frac{L-\ell}{2}} r^\ell \\ &= S^{-\frac{L}{2}} \frac{1 - (\sqrt{S}r)^L}{1 - \sqrt{S}r} \end{aligned}$$

This leads to another transtion inside the ‘‘order’’ regime: if  $\sqrt{S}r < 1$  the NTK  $\Theta_\infty^{(L,pp)}(x, x)$  goes to zero and if  $\frac{1}{\sqrt{S}} < r < 1$  it converges to a constant. If we translate the bound of Proposition 19 to the NTK with varying learning rates, the convergence to a constant is only guaranteed when  $\sqrt{S}r < 1$ , which suggests that adapting the learning (or changing the number of channels) does reduce the checkerboard artifacts (as confirmed by numerical experiments):

**Proposition 20.** *If  $r < 1$  the limiting NTK at any two inputs  $x, y$  such that for all  $p \in \mathbb{Z}$ ,  $\|x^p\| = \|y^p\| = \sqrt{n_0}$  and for any two output positions  $p$  and  $p'$ , such that  $k$  is the maximal integer in  $\{0, \dots, L-1\}$  such that  $s^k$  divides the difference  $p - p'$  then:*

$$\frac{1 - (\sqrt{S}r)^{k+1}}{1 - (\sqrt{S}r)^L} \geq \vartheta_\infty^{(L,pp')} (x, y) \geq \frac{1 - (\sqrt{S}r)^{k+1}}{1 - (\sqrt{S}r)^L} - \frac{C_{\sigma, \beta} (\sqrt{S}r)^k}{|1 - (\sqrt{S}r)^L|}$$

*Proof.* The NTK can be bounded recursively

$$\begin{aligned}\Theta_{\infty}^{(L,pp')}(x, y) &= S^{-L-1/2}\Sigma^{(L,pp')}(x, y) + \delta_{s|p-p'} \frac{1-\beta^2}{|P(p)|} \sum_{q \in P(p)} \Theta_{\infty}^{(L-1;q,q+\frac{p'-p}{s})}(x, y) R_{\hat{\sigma}} \left( \Sigma^{(L-1;q,q+\frac{p'-p}{s})}(x, y) \right) \\ &\geq S^{-L-1/2}(1-2(1-\beta^2)r^k) + \delta_{s|p-p'} \frac{1}{|P(p)|} \sum_{q \in P(p)} \Theta_{\infty}^{(L;q,q+\frac{p'-p}{s})}(x, y) (r - \psi 2(1-\beta^2)^2 r^{k-1})\end{aligned}$$

unrolling, we get

$$\begin{aligned}\Theta_{\infty}^{(L,pp')}(x, y) &\geq \sum_{m=0}^k S^{-\frac{L-k+m}{2}} (1-2(1-\beta^2)r^m) \prod_{n=m+1}^k (r - \psi 2(1-\beta^2)^2 r^{n-1}) \\ &\geq \sum_{m=0}^k S^{\frac{k-m-L}{2}} r^{k-m} - S^{\frac{k-m-L}{2}} 2(1-\beta^2)r^{k-m} r^m - S^{\frac{k-m-L}{2}} \psi 2(1-\beta^2)^2 \sum_{n=m+1}^k r^{k-m-1} r^{n-1} \\ &\geq S^{-L/2} \frac{1 - (\sqrt{S}r)^{k+1}}{1 - \sqrt{S}r} - 2 \frac{1-\beta^2}{1-S^{-1/2}} S^{\frac{k-L}{2}} r^k - \psi 2(1-\beta^2)^2 r^{k-1} \sum_{m=0}^k S^{\frac{k-m-L}{2}} \sum_{n=0}^{k-m-1} r^n \\ &\geq S^{-L/2} \frac{1 - (\sqrt{S}r)^{k+1}}{1 - \sqrt{S}r} - 2 \frac{1-\beta^2}{1-S^{-1/2}} S^{\frac{k-L}{2}} r^k - \psi 2(1-\beta^2)^2 r^{k-1} S^{\frac{k-L}{2}} \frac{1}{1-S^{-1/2}} \frac{1}{1-r} \\ &\geq S^{-L/2} \frac{1 - (\sqrt{S}r)^{k+1}}{1 - \sqrt{S}r} - 2 \frac{1-\beta^2}{1-S^{-1/2}} \left[ 1 + \frac{\psi r(1-\beta^2)}{1-r} \right] r^k S^{\frac{k-L}{2}} \\ &\geq S^{-L/2} \left( \frac{1 - (\sqrt{S}r)^{k+1}}{1 - \sqrt{S}r} - C_{\sigma,\beta} (\sqrt{S}r)^k \right)\end{aligned}$$

and for the upper bound:

$$\Theta_{\infty}^{(L,pp')}(x, y) \leq \sum_{m=0}^k S^{-\frac{L-k+m}{2}} \prod_{n=m+1}^k r = S^{-L/2} \frac{1 - (\sqrt{S}r)^{k+1}}{1 - \sqrt{S}r}.$$

Dividing by  $\Theta_{\infty}^{(L,pp)}(x, x)$  we obtain

$$\frac{1 - (\sqrt{S}r)^{k+1}}{1 - (\sqrt{S}r)^L} \geq \vartheta_{\infty}^{(L,pp')}(x, y) \geq \frac{1 - (\sqrt{S}r)^{k+1}}{1 - (\sqrt{S}r)^L} - \frac{C_{\sigma,\beta}(\sqrt{S}r)^k}{|1 - (\sqrt{S}r)^L|}$$

□

## G Border Effects

With the usual scaling of  $\frac{1}{\sqrt{|\omega/s_1 \dots s_d|}}$ , in a General ConvNet, the positions on the border have less parents and hence a lower activation variance. In this section, we show, in a special example, how this parametrization leads to border effects in the limiting activation kernels and NTK. This could be generalized to a more general setting, yet, our main purpose is to show that with the parent-based parametrization—as defined in Section E—no border artifact is present in both kernels in this general setting.

The following proposition illustrates the border artifact present in the usual NTK-parametrization. Let us consider a DC-NN with a standardized ReLU nonlinearity, with  $I_0 = I_1 \dots = \mathbb{N}$ , with up-sampling stride of 2, and windows  $\pi_0 = \omega_0 = \pi_1 = \omega_1 = \dots = \{-3, -2, -1, 0\}$ . In particular, there is only one border at position 0. Using the formalism of Section E, the set of parents of a position  $p$  is  $P(p) = \{\lfloor p/2 \rfloor - 1, \lfloor p/2 \rfloor\} \cap \mathbb{N}$ . In particular, any generic position in any hidden or last layer has 2 parents except for the border  $p = 0$  for which  $P(0) = \{0\}$ .



**Proposition 21.** *In the setting introduced above, for any  $x \in \mathbb{S}_{n_0}^{I_0}$ , the kernels satisfy:*

$$\Sigma^{(\ell,00)}(x,x) = \frac{\beta^2 + (r/2)^{\ell+1}}{1-r/2} \text{ and } \Theta_\infty^{(L,00)}(x,x) = \frac{\beta^2(1-(r/2)^L)}{(1-r/2)^2} + L \frac{(r/2)^{L+1}}{1-r/2}.$$

*In particular  $\Sigma^{(\ell,00)}(x,x)$  is smaller than the “bulk-value”  $\lim_{p \rightarrow \infty} \Sigma^{(\ell,pp)}(x,x) = 1$  and  $\Theta_\infty^{(L,00)}(x,x)$  is smaller than the “bulk-value”  $\lim_{p \rightarrow \infty} \Theta_\infty^{(L,pp)}(x,x) = \frac{1-r^L}{1-r}$ .*

*Proof.* Recall that for the standardized ReLU,  $r_{\sigma,\beta} = 1 - \beta^2$ . From now on, we denote  $r = r_{\sigma,\beta}$  and  $x$  is an element of  $\mathbb{S}_{n_0}^{I_0}$ . For any  $\ell = 0, 1 \dots$ , we have:

$$\Sigma^{(\ell+1,00)}(x,x) = \beta^2 + \frac{1-\beta^2}{2} \sum_{q \in P(0)} \mathbb{E}_{z \sim \mathcal{N}(0, \Sigma_{qq}^{(\ell)}(x,x))} [\sigma(x)^2] = \beta^2 + \frac{1-\beta^2}{2} \Sigma^{(\ell,00)}(x,x).$$

Since  $x \in \mathbb{S}_{n_0}^{I_0}$ , we get  $\Sigma^{(1)}(x,x) = \beta^2 + \frac{r}{2}$ : this implies the following equalities:

$$\begin{aligned} \Sigma^{(\ell,00)}(x,x) &= (r/2)^\ell + \sum_{k=0}^{\ell-1} \beta^2 (r/2)^k \\ &= (r/2)^\ell + \beta^2 \frac{1-(r/2)^\ell}{1-r/2} \\ &= \frac{\beta^2}{1-r/2} + \frac{(r/2)^\ell - (r/2)^{\ell+1} - \beta^2 (r/2)^\ell}{1-r/2} \\ &= \frac{\beta^2 + (r/2)^{\ell+1}}{1-r/2}. \end{aligned}$$

For the limiting NTK, with the usual NTK parametrization, the following recursion holds:

$$\Theta_\infty^{(L+1,00)}(x,x) = \Sigma^{(L+1,00)}(x,x) + \frac{r}{2} \Theta_\infty^{(L,00)}(x,x) \mathbb{L}_{\Sigma^{(L,00)}(x,x)}^{\dot{\sigma}}.$$

Note that for the standardized ReLU,  $\dot{\sigma}$  is a rescaled Heaviside, thus  $\mathbb{L}_{\Sigma^{(L,00)}(x,x)}^{\dot{\sigma}} = \mathbb{E}_{x \sim \mathcal{N}(0, \Sigma^{(L,00)}(x,x))} [\dot{\sigma}(x)^2] = 2 \mathbb{E}_{x \sim \mathcal{N}(0,1)} [\mathbb{I}_{x \geq 0}] = 1$ . This implies:

$$\begin{aligned} \Theta^{(L,00)}(x,x) &= \sum_{\ell=1}^L \Sigma^{(\ell,00)}(x,x) (r/2)^{L-\ell} \\ &= \sum_{\ell=1}^L \left( \frac{\beta^2}{1-r/2} + \frac{(r/2)^{\ell+1}}{1-r/2} \right) (r/2)^{L-\ell} \\ &= \frac{\beta^2}{1-r/2} \sum_{\ell=1}^L (r/2)^{L-\ell} + L \frac{(r/2)^{L+1}}{1-r/2} \\ &= \frac{\beta^2(1-(r/2)^L)}{(1-r/2)^2} + L \frac{(r/2)^{L+1}}{1-r/2}. \end{aligned}$$

The “bulk-values” for the activation kernels and the limiting NTK kernel can be deduced from the proof of Proposition 22. A tedious study of variation of functions allows to prove the assertion on the boundary/bulk comparison.  $\square$

As a consequence of the previous proposition, in the limits as  $\ell$  and  $L$  goes to infinity, the ratio boundary/bulk value is bounded by  $\max(1, c\beta^2)$ : the smaller  $\beta$  is, the stronger the boundary effect will be.

In the parent-based parametrization, the variance of the neurons throughout the network is always equal to 1 and the NTK  $\Theta_{\infty,pp}^{(L)}(x,x)$  becomes independent of the position  $p$ : the border artifacts disappear.

**Proposition 22.** For the parent-based parametrization of DC-NNs, if the nonlinearity is standardized,  $(\Sigma^{(L)})_{pp}(x)$  and  $(\Theta_\infty^{(L)})_{pp}(x)$  do not depend neither on  $p \in I_L$  nor on  $x \in \mathbb{S}_{n_0}^{I_0}$ .

*Proof.* Actually, we will prove the stronger statement: for any General Convolutional Network, as defined in Section E, for any standardized nonlinearity, for any  $x \in \mathbb{S}_{n_0}^{I_0}$  and any  $p \in I_L$ ,

$$\Sigma^{(L,pp)}(x, x) = 1, \quad \text{and} \quad \Theta_\infty^{(L,pp)}(x, x) = \frac{1 - r^L}{1 - r}.$$

For the activation kernels, this is proven by induction on  $\ell$ . For any  $x \in \mathbb{S}_{n_0}^{I_0}$  and any  $p \in I_1$ :

$$\begin{aligned} \Sigma^{(1,pp)}(x, x) &= \beta^2 + \frac{1 - \beta^2}{|P(p)| n_0} \sum_{q \in P(p)} \sum_{q' \in P(p)} \chi(q \rightarrow p, q' \rightarrow p) x_q^T x_{q'} \\ &= \beta^2 + \frac{1 - \beta^2}{|P(p)| n_0} \sum_{q \in P(p)} x_q^T x_q \\ &= \beta^2 + (1 - \beta^2) \\ &= 1, \end{aligned}$$

and if the assertion holds true for  $L$ , then:

$$\begin{aligned} \Sigma^{(L+1,pp)}(x, x) &= \beta^2 + \frac{1 - \beta^2}{|P(p)| n_0} \sum_{q \in P(p)} \sum_{q' \in P(p)} \chi(q \rightarrow p, q' \rightarrow p) \Sigma^{(L,qq')}(x, x) \\ &= \beta^2 + \frac{1 - \beta^2}{|P(p)| n_0} \sum_{q \in P(p)} \Sigma^{(L,qq)}(x, x) \\ &= 1. \end{aligned}$$

For the activation kernels, this is proven by induction on  $L$ . It is easy to see that  $\Theta_\infty^{(1,pp)}(x, x) = 1$  is valid for any  $x \in \mathbb{S}_{n_0}^{I_0}$  and any  $p \in I_L$ . Let us show the induction step:

$$\begin{aligned} \Theta_\infty^{(L+1,pp)}(x, x) &= \Sigma^{(L+1,pp)}(x, x) + \frac{1 - \beta^2}{|P(p)|} \sum_{q \in P(p)} \Theta_\infty^{(L,qq)}(x, x) R_\sigma \left( \Sigma^{(L,qq)}(x, x) \right) \\ &= 1 + r \Theta_\infty^{(L,qq)}(x, x). \end{aligned}$$

Thus,  $\Theta_\infty^{(L,pp)}(x, x) = \sum_{\ell=1}^L r^{L-\ell} = \frac{1-r^L}{1-r}$ .  $\square$

## H Layerwise Contributions to the NTK and Checkerboard Patterns

In a DC-NN with stride  $s \in \{2, 3, \dots\}^d$ , if two connection weight matrices  $W^{(\ell, q \rightarrow p)}$  and  $W^{(\ell, q' \rightarrow p')}$  are shared then  $s \mid p' - p$ . In other words,  $\chi(q \rightarrow p, q' \rightarrow p') = 0$  as soon as  $s \nmid p' - p$ . The limiting contribution of the weights  $\Theta_\infty^{(L; W^{(\ell)})}$  and bias  $\Theta_\infty^{(L; b^{(\ell)})}$  to the limiting NTK can be formulated recursively. For the last layer  $L - 1$  we have

$$\begin{aligned} \Theta_\infty^{(L; b^{(L-1)}, pp')} &= \beta^2 \\ \Theta_\infty^{(1; W^{(0)}, pp')} &= \delta_{s \mid p-p'} \frac{1 - \beta^2}{|P(p)| n_0} \sum_{q \in P(p)} x_q^T y_{q + \frac{p'-p}{s}} \\ \Theta_\infty^{(L; W^{(L-1)}, pp')} &= \delta_{s \mid p-p'} \frac{1 - \beta^2}{|P(p)|} \sum_{q \in P(p)} R_\sigma \left( \Sigma^{(L-1, q, q + \frac{p'-p}{s})}(x, y) \right) \text{ for } L > 1 \end{aligned}$$

and for the other layers, we have

$$\Theta_{\infty}^{(L+1:b^{(\ell)}, pp')} = \delta_{s|p-p'} \frac{1-\beta^2}{|P(p)|} \sum_{q \in P(p)} \Theta_{\infty}^{(L;b^{(\ell)}, q, q+\frac{p'-p}{s})}(x, y) R_{\dot{\sigma}} \left( \Sigma^{(L, q, q+\frac{p'-p}{s})}(x, y) \right)$$

$$\Theta_{\infty}^{(L+1:W^{(\ell)}, pp')} = \delta_{s|p-p'} \frac{1-\beta^2}{|P(p)|} \sum_{q \in P(p)} \Theta_{\infty}^{(L;W^{(\ell)}, q, q+\frac{p'-p}{s})}(x, y) R_{\dot{\sigma}} \left( \Sigma^{(L, q, q+\frac{p'-p}{s})}(x, y) \right).$$

**Proposition 23.** *In a DC-NN with stride  $s \in \{2, 3, \dots\}^d$ , we have  $\Theta_{\infty}^{(L:W^{(\ell)}, pp')}(x, y) = 0$  if  $s^{L-\ell} \nmid p' - p$  and  $\Theta_{\infty}^{(L:b^{(\ell)}, pp')}(x, y) = 0$  if  $s^{L-\ell-1} \nmid p' - p$ .*

*Proof.* From the formulas of the limiting contributions  $\Theta^{(L:W^{(\ell)})}$  and  $\Theta^{(L:b^{(\ell)})}$ , we see that the bias of the last layer contribute to all pairs  $p, p'$  while the bias only contribute to pairs such that  $s \mid p' - p$ . Now by induction on  $L$ , if  $\Theta^{(L:b^{(\ell)}, qq')}$  and  $\Theta^{(L:W^{(\ell)}, qq')}$  only contribute to pairs  $q, q'$  such that  $s^{L-\ell-1} \mid q' - q$  and  $s^{L-\ell} \mid q' - q$  then

$$\Theta_{\infty}^{(L+1:b^{(\ell)}, pp')} = \delta_{s|p-p'} \frac{1-\beta^2}{|P(p)|} \sum_{q \in P(p)} \Theta_{\infty}^{(L;b^{(\ell)}, q, q+\frac{p'-p}{s})}(x, y) R_{\dot{\sigma}} \left( \Sigma^{(L, q, q+\frac{p'-p}{s})}(x, y) \right)$$

$$\Theta_{\infty}^{(L+1:W^{(\ell)}, pp')} = \delta_{s|p-p'} \frac{1-\beta^2}{|P(p)|} \sum_{q \in P(p)} \Theta_{\infty}^{(L;W^{(\ell)}, q, q+\frac{p'-p}{s})}(x, y) R_{\dot{\sigma}} \left( \Sigma^{(L, q, q+\frac{p'-p}{s})}(x, y) \right)$$

only contribute to pairs  $p', p$  such that  $s^{L-\ell} \mid p' - p$  and  $s^{L+1-\ell} \mid p' - p$  as needed.  $\square$